
[All ETDs from UAB](#)

[UAB Theses & Dissertations](#)

2012

Electrophysiological Investigation of Rabbit Retinal Ganglion Cells

Przemyslaw Nowak
University of Alabama at Birmingham

Follow this and additional works at: <https://digitalcommons.library.uab.edu/etd-collection>

Recommended Citation

Nowak, Przemyslaw, "Electrophysiological Investigation of Rabbit Retinal Ganglion Cells" (2012). *All ETDs from UAB*. 2599.
<https://digitalcommons.library.uab.edu/etd-collection/2599>

This content has been accepted for inclusion by an authorized administrator of the UAB Digital Commons, and is provided as a free open access item. All inquiries regarding this item or the UAB Digital Commons should be directed to the [UAB Libraries Office of Scholarly Communication](#).

ELECTROPHYSIOLOGICAL INVESTIGATION OF RABBIT
RETINAL GANGLION CELLS

by

PRZEMYSŁAW NOWAK

ALLAN C. DOBBINS, CHAIR
TIMOTHY J. GAWNE
NORBERTO M. GRZYWACZ
KENT T. KEYSER
THOMAS T. NORTON

A DISSERTATION

Submitted to the graduate faculty of The University of Alabama at Birmingham,
in partial fulfillment of the requirements for the degree of
Doctor of Philosophy

BIRMINGHAM, ALABAMA

2012

ELECTROPHYSIOLOGICAL INVESTIGATION OF RABBIT RETINAL GANGLION CELLS

PRZEMYSŁAW NOWAK

NEUROSCIENCE GRADUATE PROGRAM

ABSTRACT

The retina is the first stage of the visual system, responsible for transducing light into the neural signal and for subsequent processing of this signal before sending it to the higher visual centers in the brain. The output to the higher visual centers is mediated by retinal ganglion cells, which not only relay the signal, but also substantially contribute to its processing. Depending on what computations they perform, they are subdivided into different types. These cells have been extensively studied in various species, one prominent example being the rabbit. In rabbits, one characteristic type comprises On-Off directionally selective retinal ganglion cells (On-Off DS RGCs), whose response is modulated by the direction of motion of a moving visual stimulus. These cells respond most strongly to a stimulus moving in their preferred direction and very weakly to a stimulus moving in the opposite direction, whereas intermediate directions evoke intermediate responses. However, the response is also affected by nondirectional parameters, such as speed and contrast, which confounds information on the stimulus direction and makes the response ambiguous. This raises a question of what information is actually conveyed by these cells and in what form. To address this problem, the precise relationship between various stimulus parameters and the cell response must be determined. This dissertation shows that responses of On-Off DS RGCs are multiplicatively separable: response measured as the mean spike count is a product of the effects of direction, speed, and luminance. Moreover, speed and luminance tuning curves

are similar in On-Off DS RGCs across the retina. Furthermore, it demonstrates that responses of On-Off DS RGCs involve characteristic bursts, which allow these cells to encode direction and nondirectional parameters in different aspects of the spike train. These results suggest that direction could possibly be decoded from mean spike count responses of local populations of On-Off DS RGCs, whereas the combined effect of the nondirectional parameters could be estimated from interburst intervals.

Keywords: rabbit, retina, ganglion cells, direction selectivity, neural code, visual motion.

DEDICATION

I dedicate this dissertation to my wonderful wife, Anna. Thank you for your love, encouragement, and never ending support, in good times and in bad.

ACKNOWLEDGMENTS

In this endeavor, I have received support, advice, and encouragement from many people, and I am grateful to all of them. Below I mention those few whose contribution has been the most significant.

First of all, I would like to thank my mentor, Dr. Allan Dobbins. He has been an excellent mentor, always offering the best of his knowledge and skills to train me to become a professional scientist. He has given me great guidance throughout my project while providing me, on the other hand, with much independence. His help and support have been truly extraordinary. I have been impressed by his critical thinking skills and his vast knowledge, and I have learned a great deal observing how he combines the two.

I am also grateful to my other Committee members: Dr. Timothy Gawne (co-mentor), Dr. Norberto Grzywacz, Dr. Kent Keyser, and Dr. Thomas Norton, for numerous discussions, suggestions, and comments, which guided me through my project.

I would like to thank Dr. Franklin Amthor for allowing me to use his laboratory, in which I collected all experimental data for the project, and Dr. John Tootle, who developed custom-tailored data acquisition software that made it possible.

I am deeply indebted to Dr. Lori McMahon, Director of the Neuroscience Graduate Program, for her outstanding support and encouragement. She gave me an opportunity to turn my interest in neuroscience into a professional career, has always inspired me and motivated to do my best, and was key in resolving several problems that

emerged on my way. Her enthusiasm and dedication to students make her, in my view, the role model as a program director.

Finally, I would like to thank my two colleagues and friends in the laboratory: Dr. Jordan Renna, who taught me practical retinal electrophysiology, and Dr. Michael Risner, who was always there to help me with experiments and has given me a great deal of advice not only related to science.

TABLE OF CONTENTS

	<i>Page</i>
ABSTRACT	ii
DEDICATION	iv
ACKNOWLEDGMENTS	v
LIST OF FIGURES	viii
INTRODUCTION	1
Retina	1
Retinal Ganglion Cells	3
Rabbit Retinal Ganglion Cells	5
Directionally Selective Retinal Ganglion Cells	7
Rabbit Directionally Selective Retinal Ganglion Cells	9
Model of Directional Selectivity	13
Presynaptic Mechanism	15
Postsynaptic Mechanism	18
Central Projections and Function	18
Research Question and Aims	19
SEPARABILITY OF STIMULUS PARAMETER ENCODING BY ON-OFF DIRECTIONALLY SELECTIVE RABBIT RETINAL GANGLION CELLS	25
INDEPENDENT CODING OF DIRECTION AND SPEED IN DIRECTIONALLY SELECTIVE RETINAL GANGLION CELLS	94
DISCUSSION	117
GENERAL LIST OF REFERENCES	124
APPENDIX: INSTITUTIONAL ANIMAL CARE AND USE COMMITTEE APPROVAL FORM	130

LIST OF FIGURES

<i>Figure</i>	<i>Page</i>
---------------	-------------

INTRODUCTION

1	Simplified Diagram of the Retina	21
2	Directional Selectivity in a Visual Cell	22
3	Barlow-Levick Model of Directional Selectivity	23
4	Simplified Diagram of On-Off DS RGC Connectivity.....	24

SEPARABILITY OF STIMULUS PARAMETER ENCODING BY ON-OFF DIRECTIONALLY SELECTIVE RABBIT RETINAL GANGLION CELLS

1	Direction Tuning Curves and Their Widths.....	80
2	Functional Approximation of Direction Tuning Curves.....	82
3	Invariance of Direction Tuning Curves	83
4	Speed Tuning Curves and Their Invariance.....	85
5	Functional Approximation of Speed Tuning Curves	87
6	Luminance Tuning Curves and Their Invariance	88
7	Functional Approximation of Luminance Tuning Curves.....	90
8	Prediction of Spike Count when Direction, Speed, and Luminance Are Covaried.....	91
9	Prediction of Spike Count for a Population of Cells in which Direction, Speed, and Luminance Are Covaried	92
10	Invariance of Direction Tuning Curves with Respect to Sign of Contrast	93

INDEPENDENT CODING OF DIRECTION AND SPEED IN DIRECTIONALLY SELECTIVE RETINAL GANGLION CELLS

1	On-Off DS Cell Response to Motion.....	110
2	Interburst Interval Decreases with Increasing Speed.....	112
3	Doublet Pattern Is Invariant with Direction.....	114
4	Effect of Speed and Direction on Spike Pattern	116

DISCUSSION

1	Direction Prediction by the Population Vector.....	123
---	--	-----

INTRODUCTION

Retina

The retina, a neural tissue lining the back of the eye, is the first stage in visual processing. It performs three major functions: first, it converts light energy into neural signals; second, it processes those signals with the goal of detecting basic features or spatiotemporal frequencies in the encoded visual image; and third, it sends the initially processed signals for further processing to the higher visual centers in the brain (Rodieck 1998).

To perform these functions, retina assumes a layered structure (Fig. 1), in which cells and their connections are arranged in two-dimensional arrays stacked upon each other (Masland 2001; Rodieck 1998; Wässle 2004). Cells that capture light and transduce it into the neural signal are called photoreceptors. There are two types of classical photoreceptors: rods, which mediate scotopic (dim light) vision, and cones, which mediate photopic (bright light) vision as well as permit color perception. Both types of photoreceptors consist of two segments: an outer segment, involved in capturing light, and an inner segment, comprising the cell body. As a result, these photoreceptors occupy two retinal layers: the outer segments constitute the photoreceptor layer, while the inner segments constitute the adjacent outer nuclear layer. The next layer, the outer plexiform layer, contains a dense network of synapses connecting photoreceptors and two classes of interneurons: bipolar cells and horizontal cells. Cell bodies of these two classes of

interneurons as well as of another class, amacrine cells, are localized to the subsequent layer, the inner nuclear layer. Another dense meshwork of synapses, this time contacting bipolar, amacrine, and retinal ganglion cells, constitutes the next, inner plexiform layer. The following layer, the ganglion cell layer, contains cell bodies of retinal ganglion cells and displaced amacrine cells (that is amacrine cells whose somas are not localized to the inner nuclear layer). In this layer, the third type (apart from rods and cones) of photoreceptors occurs, namely intrinsically photosensitive retinal ganglion cells, but they are involved in controlling the circadian rhythm rather than vision. Retinal ganglion cells project their axons to the higher visual centers in the brain, and these axons form the adjacent nerve fiber layer in the retina. Apart from the above, other retinal layers are also distinguished, yet they are not directly involved in processing visual signals, but rather have a structural and supportive role. They include the retinal pigment epithelium, the external limiting membrane, and the inner limiting membrane.

As a result of the layered structure, neural signals within the retina are routed along vertical and horizontal pathways (Masland 2001). The vertical pathway is the shortest route connecting photoreceptors and retinal ganglion cells via bipolar cells. It comprises different information channels, which can be distinguished along two dimensions. The first dimension concerns the polarity of light: On bipolar cells increase their responses with light increments, whereas Off bipolar cells increase their responses with light decrements. The second dimension, in turn, deals with temporal domain: one group of bipolar cells codes high frequency components of the visual signal (transient information), while the other group codes low frequency components (sustained information). On the other hand, there are two horizontal pathways: the first one involves

horizontal cells, which contact photoreceptors, and the other one involves amacrine cells, which contact both bipolar and ganglion cells. Each horizontal pathway mediates lateral inhibition, a phenomenon critical to the signal processing performed in the retina.

Retinal Ganglion Cells

Retinal ganglion cells (RGCs) constitute the output cells of the retina. However, they are not simple relay cells, but rather are heavily involved in the signal processing that the retina carries out. One form of this processing may consist in spatiotemporal filtering, with cells modulating responses depending on the particular spatial and temporal frequencies present in the visual image falling on their receptive fields, which subserves Fourier analysis. Another form comprises feature detection, with cells responding selectively to distinctive features of the stimulus present in their receptive fields, such as the direction of motion.

The receptive field of a visual cell corresponds to the region of retina (or, equivalently, to the region of field of view) in which the presence of a stimulus generates or modulates the cell response (Hartline 1938; Levick 1972; Rodieck 1998). The concept and first classification of receptive fields of RGCs was contributed by Hartline (1938). When recording from axons of individual RGCs in the optic nerve in the frog, he observed that they could be assigned to one of three groups depending on the responses to a flash of light: the first group exhibited only On responses, the second group exhibited only Off responses, and the third group exhibited both On and Off responses. These findings were later confirmed by Barlow (1953), who also made a new observation: when the stimulus size was increased beyond the central receptive field area into the annular

surrounding region, cell responses decreased, indicating an inhibitory effect of the surround. About the same time, when recording from cat RGCs, Kuffler (1953) independently discovered that their receptive fields have a center-surround organization, consisting of two concentric regions: an approximately circular central region surrounded by an annulus, with the two regions interacting with each other. He observed the same phenomenon as Barlow (1953), confirming the excitatory role of the center and the inhibitory role of the surround, and, moreover, he found that a stimulus confined to the surround can also evoke a response provided that the stimulus is of the opposite contrast to that corresponding to the cell category (for instance, a dark annulus in the case of an On RGC). Consequently, the classification proposed by Hartline (1938) has been associated with the behavior of the receptive field center. Numerous later studies, however, have demonstrated that although all surrounds are inhibitory, the presence of an opposite contrast stimulus in the surround by itself does not always yield the effect described by Kuffler (1953): in some RGCs it evokes responses, but in others it does not. Therefore, surrounds have been divided into antagonistic and silent (also termed suppressive) (Levick 1972), *antagonistic* referring to those exhibiting such response and *silent* referring to those lacking it. As a result, a silent surround can be detected only when an appropriate contrast stimulus extends beyond the center, in which case the response becomes attenuated.

The center-surround organization of the receptive fields of RGCs emerges from various mechanisms, a number of which exist prior to RGCs in the processing pathway. One originates in the outer plexiform layer owing to the lateral inhibition mediated by horizontal cells, which provide inhibitory feedback to photoreceptors such that the

resulting response of each bipolar cell reflects the ratio between the light intensities incident on the photoreceptors contacted by the bipolar cell and those incident on the neighboring area (Werblin and Dowling 1969). Bipolar cells also support this organization by splitting the signals from photoreceptors into separate On and Off channels. One implication of this split in the inner plexiform layer is that bipolar cells from the two channels make synaptic contacts with RGCs at different levels: those in the Off channel contact RGCs exclusively in the distal (Off) sublamina, whereas those in the On channel contact RGCs in the proximal (On) sublamina. In addition, amacrine cells in the inner plexiform layer contribute to lateral inhibition and the center-surround organization (Werblin 1972). Amacrine cells, moreover, are essential for the complex feature selection exhibited by RGCs.

The above general characterization does not fully describe the variety of RGCs. There are many different types of these cells, and they can be categorized based on a multitude of criteria related to their morphology, genetic and molecular markers, synthesized neurotransmitters, expressed receptors, and exhibited physiological properties. Furthermore, some types of RGCs occur universally across species, but some are species-specific. The underlying question, however, remains the same: what specific functions does each cell type performs, and in what computations is it involved?

Rabbit Retinal Ganglion Cells

Mammalian retinal ganglion cells have been investigated in several species, one of the most extensively studied being the rabbit (see Levick 1972). In rabbits, RGCs are divided into two major categories: those with concentric receptive fields and those with

complex receptive fields, and each category is subject to further subdivision (Barlow et al. 1964).

Concentric RGCs have the classical center-surround form, and their surround is antagonistic (Barlow et al. 1964; Caldwell and Daw 1978). They can be classified depending on various response properties: brisk vs. sluggish (how rapidly the response occurs), sustained vs. transient (how long the response persists), nonlinear vs. linear (whether the response is affected by a change in the distribution of light in the receptive field center when the amount of light stays constant) (Amthor et al. 1989a; Caldwell and Daw 1978). There are many different types of concentric RGCs, as described by combinations of those properties, the most prominent being brisk-sustained-linear, brisk-sustained-nonlinear, brisk-transient-linear, sluggish-sustained-linear, and sluggish-transient-nonlinear.

Complex RGCs are selective to complex stimulus features (Amthor et al. 1989b; Barlow et al. 1964; Levick 1967), but the particular form of the trigger feature cannot be predicted from responses to flashing stimuli. Complex RGCs include On and On-Off directionally selective RGCs, whose responses are modulated by the direction of stimulus motion; orientation selective cells, which respond preferentially to specific orientations of lines and edges; local edge detectors, which signal presence of a stopped (local) edge in their receptive fields; and uniformity detectors, characterized by high maintained firing in steady light, which becomes quenched with any change in the light pattern incident on their receptive fields. Unlike in the case of concentric RGCs, the surrounds of these cells are suppressive (with the exception of the uniformity detector, in which the whole receptive field is suppressive).

Directionally Selective Retinal Ganglion Cells

One type of complex RGCs in rabbits that has been extensively studied because of its distinct properties is the On-Off directionally selective RGC (see Demb 2007; Vaney et al. 2012), and these cells are the subject of this dissertation. They belong to a broader category of directionally selective (DS) cells, which are ubiquitous in the nervous system.

In general, DS cells modulate their responses with respect to the direction of motion (Fig. 2), which, depending on the part of the nervous system, can be either sensed (as in the visual system) or performed (as in the motor system). Because their responses are asymmetrical, these cells are characterized by the preferred-null axis: the preferred direction is the one in which the cell fires most vigorously, while the opposite direction, termed null (or antipreferred), elicits minimal response. Intermediate directions between these two extremes yield intermediate responses, gradually decreasing as the direction changes from the preferred to the null.

DS cells are found in diverse systems in most species. For example, the cercal sensory system of the cricket contains neurons devoted to signaling the wind direction (Miller et al. 1991); the sensory system of the medicinal leech contains neurons signaling the location of a light touch stimulus on the body wall, which mediate the local bend reflex (Lewis and Kristan 1998); and the motor cortex of the monkey contains neurons signaling the direction of an arm movement (Georgopoulos et al. 1982).

The role of DS cells in the visual system is to signal the direction of motion of a visual stimulus. This information is important for numerous reasons, and it deals with both local and global motion (Borst and Euler 2011). Local motion in the visual image

occurs when a local object is moving against its background. Information on direction of such motion may be crucial for survival because it may be related to an approaching predator that should be avoided or to escaping prey that should be captured. On the other hand, global motion occurs when the whole visual image is moving, and its most prominent example is optic flow. Optic flow (termed also optical flow) refers to motion of the image due to a movement of the observer through the environment (Bremmer 2008; Harris 1994; Lappe et al. 1999; Mallot 2000). Optic flow contains a large amount of information concerning the observer's own movement, such as translation and rotation, as well as concerning the three-dimensional structure of the surrounding world, and thus is essential for visually guided behavior and especially locomotion. It comprises cues on heading, that is the direction in which the observer is moving, whose assessment is critical for navigation; cues on how to perform image segmentation, necessary to separate objects in the visual image; cues concerning depth, used to assess the relative positions of those objects; and cues for estimation of time to contact (termed also time to collision), that is the time that remains to reach or hit an object, which is critical for obstacle avoidance. All of this information can be estimated when optic flow is processed by the visual system, which presumably requires, as the first step, assessment of the global velocity field, that is quantification of the direction and speed of motion of every point in the visual image. It should be noted, however, that estimation of some of this information (such as information on depth) may not necessitate assessment of the global velocity field, but instead can possibly be performed using only direction field or discontinuities in the velocity field.

Visual DS cells are present across many species, both vertebrate and invertebrate (Borst and Euler 2011), and they occur at different levels of processing, both cortical and subcortical (Elstrott and Feller 2009). In several species, namely in the frog (Maturana et al. 1960), rabbit (Barlow and Hill 1963), pigeon (Maturana and Frenk 1963), goldfish (Jacobson and Gaze 1964), squirrel (Michael 1966), cat (Stone and Fabian 1966), turtle (Lipetz and Hill 1970), salamander (Werblin 1970), goat (Hughes and Whitteridge 1973), mouse (Yoshida et al. 2001), and rat (Sun et al. 2011), they have been identified as early as in the retina.

Rabbit Directionally Selective Retinal Ganglion Cells

In rabbits, there are three types of RGCs that exhibit directional selectivity: two types of On DS RGCs (Hoshi et al. 2011; Kanjhan and Sivyer 2010) and one type of On-Off DS RGCs (Barlow and Hill 1963). The two types of On DS RGCs are called, respectively, transient On DS RGCs, since they produce brief responses to a stationary spot of light flashed in their receptive field, and sustained On DS RGCs, because their responses to such a stimulus are longer. On DS RGCs and On-Off DS RGCs differ in several important aspects. The first one concerns how they respond to stationary stimuli and is related to their names: On DS RGCs respond only to light increments (and thus bright objects), whereas On-Off DS RGCs respond to both light increments and decrements (and thus both bright and dark objects) (Barlow et al. 1964). However, this also has implications for moving stimuli: when a bright bar traverses the receptive field, On DS RGCs respond only to the leading edge, while On-Off DS RGCs respond both to the leading and the trailing edges (Barlow et al. 1964). Speed is another distinguishing

factor: On DS RGCs respond only when the stimulus is moving at slow speeds, whereas On-Off DS RGCs respond to a much broader range of speeds (Oyster 1968; Wyatt and Daw 1976). Several further differences pertain to the properties of the receptive fields. The receptive fields of On DS RGCs are much larger than those of On-Off DS RGCs (Amthor et al. 1989b). On DS RGCs have a weak inhibitory surround, so they respond best to global motion spanning the whole of their receptive field. In contrast, On-Off DS RGCs exhibit a strong inhibitory surround, so they respond best to local motion confined to the receptive field center. On DS RGCs and On-Off DS RGCs also differ in morphology, distributions of their preferred directions, and central projections (see Vaney et al. 2012).

Rabbit On-Off DS RGCs were first described by Barlow and Hill (1963), who observed robust asymmetry in their responses to a spot of light moving in opposite directions, independent of the sign and magnitude of contrast. In a subsequent study, Barlow et al. (1964) mapped responses to a range of directions, and showed that the response decreases gradually between the preferred and null directions. They also noticed that the cell maintains its directionally selective character over a wide range of speeds. Barlow and Levick (1965) found that directional selectivity is exhibited throughout the receptive field, and can be elicited for motion extent as little as 0.25° , regardless of the stimulus initial position. They also observed that the directional selectivity can be obtained with gratings. The robustness of directional selectivity of On-Off DS RGCs has been thoroughly confirmed by Grzywacz and Amthor (2007), who showed that these cells remain directionally selective independent of many nondirectional stimulus

parameters, namely sign and amount of contrast, spatial configuration, spatial frequency, speed, and motion extent.

Apart from robustness of directional selectivity, other properties of On-Off DS RGCs have also been determined. Their responses to stationary spots are brisk (Caldwell and Daw 1978) and transient (Levick 1967). Spontaneous activity is usually low (Ariel and Daw 1982a), and in those cells in which it is somewhat higher motion in the null direction would suppress it (Barlow et al. 1964). Preferred directions are the same for both positive (On) and negative (Off) contrast stimuli (Barlow and Hill 1963; Amthor et al. 1989b; Taylor and Vaney 2002). Additionally, On and Off receptive field centers overlap and are nearly coextensive, although in some cells responses to On vs. Off stimuli may not be of equal magnitude and thus one of them may dominate (Amthor et al. 1989b). There is evidence that the On and Off channels can operate independently (Cohen and Miller 1995; Kittila and Massey 1995), but, on the other hand, they share the same spike generating mechanism at the axon initial segment of the On-Off DS RGC. The surround of these cells is suppressive: both On and Off responses become reduced when the stimulus present in the center extends to the surround (Barlow et al. 1964; Barlow and Levick 1965; Amthor et al. 1989b). Moreover, surround suppression exhibits contextual effects for moving stimuli because it is largest when the stimuli in the center and in the surround match in phase as well as in spatial and temporal frequencies, but is smaller when a discontinuity between the center and the surround in any of these characteristics exists (Chiao and Masland 2003). On-Off DS RGCs have a preference for a particular spatial frequency rather than speed (Grzywacz and Amthor 2007; He and Levick 2000). The optimum spatial frequency, as measured for gratings, is such that the

leading and trailing edges are offset by the size of the receptive field, thus the traversal of either of them through the receptive field does not interfere with the traversal of the other (He and Levick 2000). Furthermore, stimulus size also affects responses, since they are stronger for small spots and weaker for small bars, even if the bars are short enough to fit into the receptive field center (Wyatt and Daw 1975).

It has been found that the preferred directions On-Off DS RGCs are not uniformly distributed, but rather cluster into four groups, corresponding to the anterior, posterior, superior, and inferior motion in the field of view, respectively (Oyster 1968; Oyster and Barlow 1967). Consequently, four subtypes of On-Off DS RGCs have been distinguished, each associated with a different cardinal direction. However, the preferred direction cannot be predicted from the cell receptive field map obtained for stationary flashing spots (Barlow and Levick 1965) or from the shape or pattern of the dendritic arborizations (Amthor et al. 1989b). Each subtype has been shown to tile the retina precisely, that is to cover the whole retina with no gaps or overlap between neighboring cells, and independently, with the four tilings not being in register with one another (Amthor and Oyster 1995; Vaney 1994).

On-Off DS RGCs have a complex morphology (Amthor et al. 1984, 1989b; Oyster et al. 1993; Yang and Masland 1994). They are bistratified — their dendritic tree forms two arborizations in the inner plexiform layer: one in the On sublamina and the other in the Off sublamina. The stratification is narrow because both arborizations are highly planar, but their shape and extent are not identical, which explains why the overlap of the On and Off receptive fields is not perfect. The diameter of the excitatory receptive field center varies between 200–300 μm in the central retina and $>600 \mu\text{m}$ in the

periphery (Yang and Masland 1994). Dendrites are thin and bear spines all over the dendritic field. Furthermore, the dendritic field resembles an irregular lattice: numerous short terminal dendrites form a large number of nearly enclosed dendritic loops throughout it, with a loop diameter of about 10–15 μm . Additionally, dendrites of overlapping On-Off DS RGCs of different subtypes cofasciculate (Amthor and Oyster 1995; Vaney 1994). The cell soma is classified as medium to large, with an average area of $\sim 150 \mu\text{m}^2$, and is placed eccentrically with respect to both sublamina arborizations of the dendritic tree.

Model of Directional Selectivity

The mechanism of directional selectivity of On-Off DS RGCs is not trivial. Because these cells exhibit directional selectivity everywhere in their receptive fields and because a movement as small as 0.25° along the preferred-null axis is enough to reveal it, the underlying mechanism must involve a large number of directionally selective subunits of the size approximately matching the minimal motion extent, reduplicated many times to cover the whole receptive field. Moreover, as Barlow and Levick (1965) reported, the null direction inhibition is strongest for small separations between two excited points (yet necessarily greater than the above threshold), and it declines when the separation exceeds 0.5° . Consequently, the mechanism must also involve interaction among subunits, which should be strongest for neighboring subunits and become weaker with an increase in the distance.

Based on these observations, Barlow and Levick (1965) proposed the first computational model explaining directional selectivity in On-Off DS RGCs (Fig. 3). The

model consists of two detectors that are separated in space and connected to logic gates, and two mechanisms: an excitatory one, facilitating the response to the preferred direction, and an inhibitory one, suppressing the response to the null direction. In the excitatory mechanism, the output of the detector on the null side (the side first encountered during null direction motion) is directly connected to the ‘And’ (conjunction) gate, whereas the output of the detector on the preferred side (the side first encountered during preferred direction motion) is connected to the same gate through a delay line. As the stimulus is moving in the preferred direction, it becomes first detected by the detector on the preferred side and after a brief delay by the detector on the null side. This temporal delay in stimulus detection by the second detector is offset by the propagation delay of the signal from the first detector to the gate. Consequently, signals from both detectors arrive at the gate simultaneously, where they are combined by the conjunction operator, and a strong response occurs. The inhibitory mechanism, in turn, is almost mirror-symmetric, except that it employs the ‘And Not’ (veto) gate. The stimulus moving in the null direction is first detected by the detector on the null side, which sends its signal to the gate through a delay line, and then detected by the detector on the preferred side, which sends its signal to the same gate without delay. Again, these two signals coincide at the gate, but by virtue of the ‘And Not’ operator the signal from the detector on the null side cancels (vetoes) that from the detector on the preferred side, and no response follows. This model, to some extent, appears as a simplified, asymmetrical version of the Reichardt detector (Reichardt 1961), a standard, biologically plausible, correlational model developed for detecting motion (Borst and Euler 2011). However, because the Reichardt detector is based on correlation, it can be associated only with the

excitatory mechanism (Barlow and Levick 1965). Barlow and Levick (1965) have argued that although there is evidence that On-Off DS RGCs employ both mechanisms proposed in their model, the effects of the inhibitory mechanism seem more pronounced than those of the excitatory counterpart, and consequently they favored inhibition as the more important constituent. Their model has received support from Wyatt and Daw (1975), who observed that for a particular spot in the receptive field inhibition comes from a cardioid-like region that extends for some distance toward the preferred direction and for smaller distances to directions at increasing angles to the preferred one, but that does not extend toward the null direction. These findings also explain why spots or short bars are more salient stimuli than long bars, an implication of the fact that the latter overlap with the inhibitory region to a larger degree. Later studies investigating synaptic inputs of On-Off DS RGCs have provided further evidence validating the model.

Presynaptic Mechanism

The On-Off DS RGC receives two types of inputs (Fig. 4): excitatory, mediated by glutamate (Massey and Miller 1990) and acetylcholine (ACh) (Masland and Ames 1976), and inhibitory, mediated by gamma-aminobutyric acid (GABA) (Merwine et al. 1998). The glutamatergic excitatory inputs come from the vertical pathway, that is from bipolar cells, whereas cholinergic excitatory inputs come from a horizontal pathway, namely from a particular type of amacrine cells called starburst amacrine cells (SACs). The GABAergic inhibitory input, in turn, comes from the same SACs, the only cells in the retina that release two neurotransmitters. Compared with bipolar cells, which are small-field, SACs are wide-field cells with radially extending dendrites, and their

dendritic fields massively overlap: each point in the retina is covered by 20–70 of them (Famiglietti 1983; Tauchi and Masland 1984). Consequently, an individual On-Off DS RGC makes many more synapses with SACs than with bipolar cells.

Excitatory and inhibitory inputs have different spatial and temporal characteristics (Fried et al. 2002; Fried et al. 2005; Lee et al. 2010; Taylor and Vaney 2002). The excitatory part of the receptive field overlaps with the dendritic tree of the On-Off DS RGC, but the inhibitory part is wider and shifted toward the null side. Moreover, inhibition is relatively delayed and prolonged. Asymmetry is further augmented because both excitatory and inhibitory inputs exhibit directional selectivity. When the stimulus is moving in the preferred direction, a large excitatory input is followed by a small inhibitory input, but the inhibition arrives too late to affect the excitation. In contrast, when the stimulus is moving in the null direction, a small excitatory input coincides with a large inhibitory input, resulting in the inhibition canceling the excitation. This variation indicates that part of the DS mechanism is already presynaptic to On-Off DS RGCs.

A critical role in shaping excitatory and inhibitory inputs to On-Off DS RGCs is performed by SACs, which provide the necessary lateral inhibition. These cells form two populations: one mediating Off responses (Off SACs), with somas in the inner nuclear layer and dendrites extending in the Off sublamina of the inner plexiform layer, and the other mediating On responses (On SACs), with somas in the ganglion cell layer and dendrites extending in the On sublamina of the inner plexiform layer (Famiglietti 1983). In both cases, SAC dendrites cofasciculate with dendrites of On-Off DS RGCs (Famiglietti 1992, Fried et al. 2002), which allows a close interaction between these two cell types. SACs release both of their neurotransmitters, GABA and ACh, on On-Off

DS RGCs (Lee et al. 2010), but synaptic connections regarding these two neurotransmitters are different. Synapses mediating GABA are localized asymmetrically on dendrites of On-Off DS RGCs, populating the null side but not the preferred side, and consequently light-evoked GABA input to On-Off DS RGCs is anisotropic (Lee et al. 2010), inhibiting response to the null direction. In contrast, synapses mediating ACh are localized symmetrically, but surprisingly light-evoked ACh input is also anisotropic, facilitating response to the preferred direction, which suggests that asymmetry occurs on functional rather than anatomical level (Lee et al. 2010). Of these two inputs, the major contribution is provided by GABA. Blocking GABA always abolishes direction selectivity (Caldwell et al. 1978; Kittila and Massey 1995; Wyatt and Daw 1976), whereas blocking ACh usually does not, but instead only reduces responses isotropically (Ariel and Daw 1982b; Kittila and Massey 1997). However, in some conditions ACh input appears essential as well, especially in the case of complex pattern stimuli, for which blocking ACh also destroys direction selectivity (Grzywacz et al. 1998). The crucial role of SACs is further demonstrated by their ablation, which results in elimination of direction selectivity in On-Off DS RGCs too (Amthor et al. 2002). The critical interactions between SACs and On-Off DS RGCs on the one hand, and the high density as well as extensive overlap of SACs on the other, suggest that SACs may subserve the high density of subunits in the receptive fields of On-Off DS RGCs.

It has been shown that both excitatory inputs, those mediated by glutamate and by ACh, are directionally selective (Fried et al. 2005; Lee et al. 2010). A putative mechanism giving rise to directional selectivity of glutamate release from bipolar cells, however, would need to be extremely intricate, which results in a disagreement on

whether it is conceivable (Fried et al. 2005; Lee et al. 2010) or, conversely, direction selectivity of glutamatergic inputs might rather be explained as an artifact observed because of a systematic recording error (Vaney et al. 2012).

Postsynaptic Mechanism

Apart from the presynaptic mechanisms giving rise to directional selectivity of On-Off DS RGCs, a postsynaptic mechanism also exists. It involves dendritic spikes (Oesh et al. 2005) and proves necessary when the stimulus motion is limited to a small portion of the receptive field. In such a case the corresponding postsynaptic potential is too weak to elicit a somatic spike, yet when it becomes converted to a dendritic spike, transmission becomes reliable. This happens because the magnitude of the dendritic spike is substantially larger than that of the postsynaptic potential, and thus the arrival of the dendritic spike at the soma is faithfully followed by an action potential. Consequently, this mechanism enables On-Off DS RGCs to reliably transmit information even when motion is confined to single subunits.

Central Projections and Function

Central projections are an important feature characterizing RGCs because they are highly related to the function that a particular type of these cells performs. In the case of On-Off DS RGCs, it has been shown that they project to various subcortical structures: lateral geniculate nucleus (Pu and Amthor 1990b), which is a relay station en route to the primary visual cortex; superior colliculus (Pu and Amthor 1990a; Vaney et al. 1981), which is involved in directing behavior toward specific objects; and nucleus of the optic

tract (Pu and Amthor 1990a), a part of the pretectal area that mediates pursuit eye movements.

However, despite their extensively studied characteristics, the function of On-Off DS RGCs in vision has not yet been agreed upon. Because these cells are sensitive to local motion, it has been hypothesized that they may be involved in detecting predators (Caldwell and Daw 1978; Famiglietti 2005). On the other hand, the preferred directions of the four subtypes align with the lines of action of the four rectus muscles in the rabbit, that is extraocular muscles producing eye movements which result in shifts of the visual axis with little or no torsional components. Therefore, these cells can be involved in eye movement control: their directional responses could signal retinal slip along the four cardinal directions, in which case its reduction would be easily achieved owing to the simple connections to the rectus muscles (Oyster 1968). This hypothesis is congruent with the fact that On-Off DS RGCs project to the nucleus of the optic tract, but importantly, both hypotheses are not mutually exclusive. However, it is possible that these cells also underlie other functions, not yet identified.

Research Question and Aims

Lack of agreement on the function of On-Off DS RGCs is further aggravated by the fact that although these cells robustly maintain directional selectivity independent of other nondirectional stimulus parameters, the nondirectional parameters also affect cell responses. For instance, it has been shown that the response in the preferred direction is contrast dependent: as contrast increases from minimum up to the optimal value, so does the response, but further increase in contrast can reduce the response (Merwine et al.

1998). A similar nonlinear relationship has been found with respect to speed (Wyatt and Daw 1975). As a result, an important question arises: what information on the stimulus do On-Off DS RGCs actually transmit and how is this information encoded?

One hypothetical possibility is that On-Off DS RGCs convey information on stimulus velocity, that is both direction and speed. This information, in turn, may be used by the higher visual centers in the brain to estimate the global velocity field and thus contribute to optic flow computations.

In pursuit to elucidate what information on the stimulus is conveyed by On-Off DS RGCs, the precise effect of both direction and nondirectional parameters on the response should be determined. This dissertation addresses the above problem.

In the first study, the effects of several stimulus parameters, namely direction, speed, luminance, and contrast, on a first-order measure of response, the mean spike count, were investigated. Both the individual and combined effects of these parameters were examined. This study also asked whether the effects of these parameters are universal throughout the retina or whether local variations exist.

In the second study, the effects of direction, speed and luminance were investigated using a second-order measure of responses, the interspike intervals. The aim of this study was to find out whether a second-order measure conveys additional information on stimulus parameters beyond what can be derived from the first-order measure.

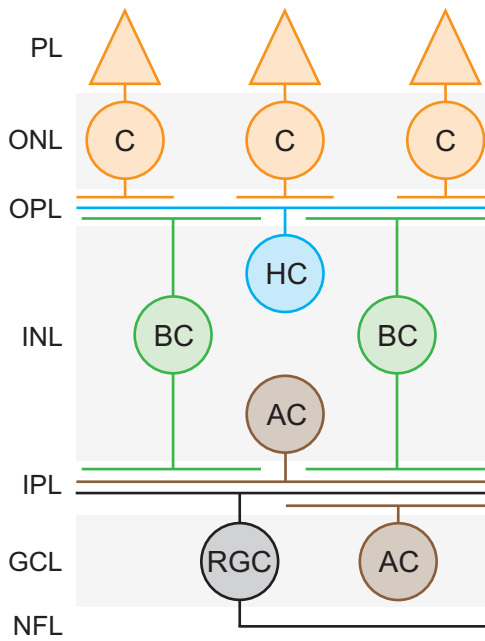


Figure 1. Simplified diagram of the retina.

Light is captured by the outer segments of photoreceptors (triangles) and converted to the neural signal, which passes along the vertical pathway comprising photoreceptors (orange), bipolar cells (green), and retinal ganglion cells (black), whose axons project to the higher visual centers. When processed along this route, the signal is also modulated by two horizontal pathways, one involving horizontal cells (blue) and the other amacrine cells (brown). Abbreviations: AC, amacrine cell; BC, bipolar cell; C, cone; GCL, ganglion cell layer; HC, horizontal cell; INL, inner nuclear layer; IPL, inner plexiform layer; NFL, nerve fiber layer; ONL, outer nuclear layer; OPL, outer plexiform layer; PL, photoreceptor layer; RGC, retinal ganglion cell. Only cones are shown; rods have been omitted for clarity.

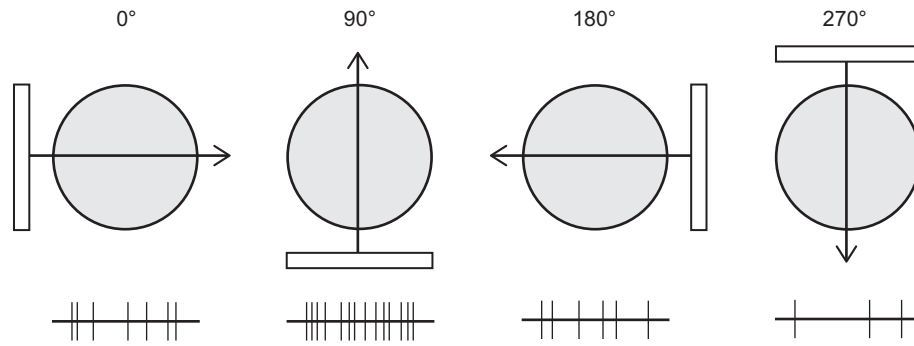


Figure 2. Directional selectivity in a visual cell.

Bar stimulus (white rectangle) traverses the cell receptive field (gray circle) in 4 cardinal directions (indicated by arrows), and corresponding cell responses are shown below. Maximum number of spikes is obtained for the upward direction (preferred), minimum number of spikes for the downward direction (null), whereas rightward and leftward directions elicit intermediate responses.

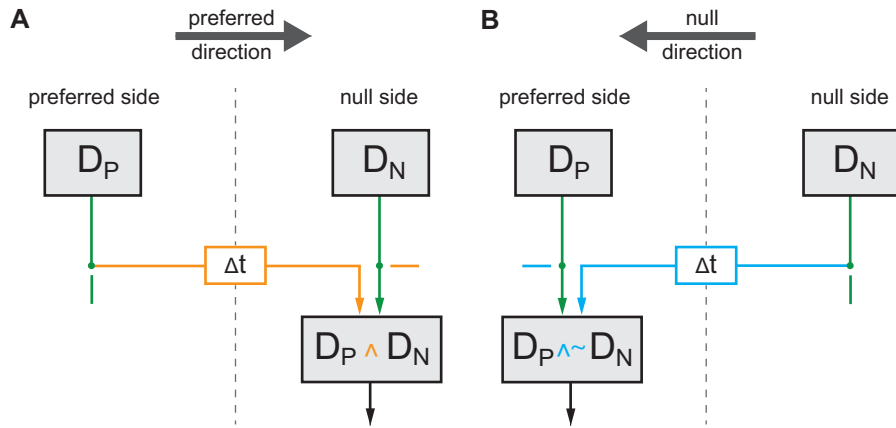


Figure 3. Barlow-Levick model of directional selectivity.

A. Excitatory mechanism facilitating response to the preferred direction. A moving stimulus activates first the detector on the preferred side (D_P) and after a delay the detector on the null side (D_N). Signals from both detectors arrive at the 'And' gate simultaneously because of the propagation delay in the signal from D_P detector, and thus a response follows.

B. Inhibitory mechanism suppressing response to the null direction. A stimulus activates first the detector on the null side and then on the preferred side, and due to the propagation delay in the signal from D_N detector the two signals arrive at the 'And Not' gate simultaneously, where they are cancelled.

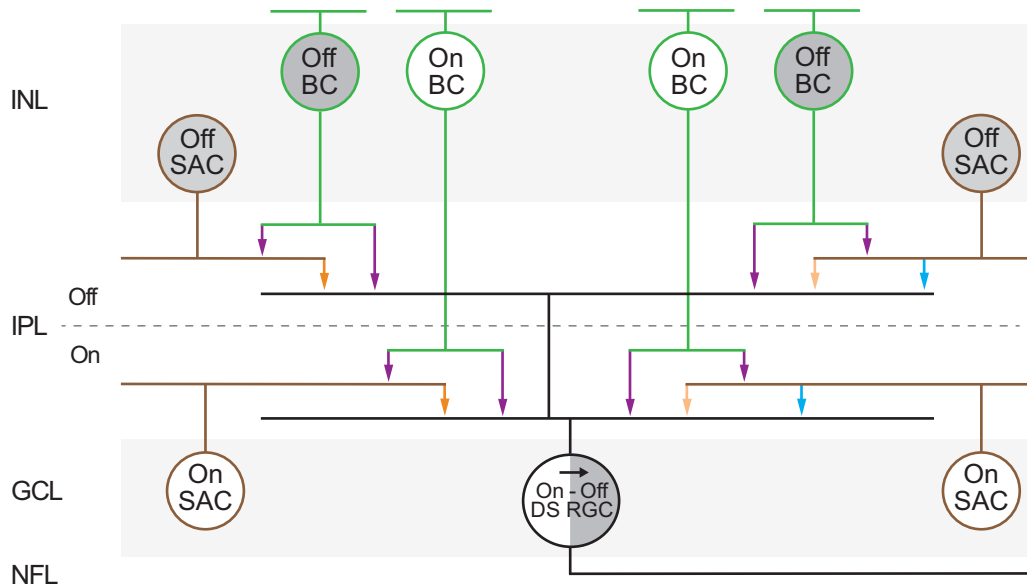


Figure 4. Simplified diagram of On-Off DS RGC connectivity.

On-Off DS RGC (black, arrow indicates preferred direction) extends dendrites to both On and Off IPL sublaminae, where they are contacted by On and Off bipolar cells, respectively, and On and Off SACs, respectively. Bipolar cells (green) release glutamate through excitatory synapses (purple arrows) on both On-Off DS RGC and SACs. SACs (brown) make inhibitory synapses (blue arrows) with On-Off DS RGC only on the null side, through which they release GABA. They also make cholinergic excitatory synapses (orange arrows) on both the preferred and null side, but release ACh only on the preferred side (depicted as darker shade of orange). Abbreviations are the same as in Figure 1 and text. Synapses between SACs have been omitted for clarity.

SEPARABILITY OF STIMULUS PARAMETER ENCODING BY ON-OFF
DIRECTIONALLY SELECTIVE RABBIT RETINAL GANGLION CELLS

by

PRZEMYSŁAW NOWAK, ALLAN C. DOBBINS, TIMOTHY J. GAWNE,
NORBERTO M. GRZYWACZ, FRANKLIN R. AMTHOR

Journal of Neurophysiology 105: 2083–2099

Copyright

2011

by

The American Physiological Society

Used by permission

Format adapted for dissertation

ABSTRACT

The ganglion cell output of the retina constitutes a bottleneck in sensory processing in that ganglion cells must encode multiple stimulus parameters in their responses. Here we investigate encoding strategies of On-Off directionally selective retinal ganglion cells (On-Off DS RGCs) in rabbits, a class of cells dedicated to representing motion. The exquisite axial discrimination of these cells to preferred vs. null direction motion is well documented: it is invariant with respect to speed, contrast, spatial configuration, spatial frequency, and motion extent. However, these cells have broad direction tuning curves and their responses also vary as a function of other parameters such as speed and contrast. In this study, we examined whether the variation in responses across multiple stimulus parameters is systematic, that is the same for all cells, and separable, such that the response to a stimulus is a product of the effects of each stimulus parameter alone. We extracellularly recorded single On-Off DS RGCs in a superfused eyecup preparation while stimulating them with moving bars. We found that spike count responses of these cells scaled as independent functions of direction, speed, and luminance. Moreover, the speed and luminance functions were common across the whole sample of cells. Based on these findings, we developed a model that accurately predicted responses of On-Off DS RGCs as products of separable functions of direction, speed, and luminance ($r = 0.98$, $P < 0.0001$). Such a multiplicatively separable encoding strategy may simplify the decoding of these cells' outputs by the higher visual centers.

INTRODUCTION

On-Off directionally selective retinal ganglion cells (On-Off DS RGCs) in rabbits were originally identified as having robustly asymmetrical responses to stimuli moving in opposite directions (Barlow and Hill 1963). They fire most vigorously when the stimulus is moving in one particular (preferred) direction, very little or not at all when it is moving in the opposite (null or antipreferred) direction, and produce responses between these two extremes for intermediate directions (Barlow et al. 1964). This distinctive directional selectivity lead to the direction of motion being referred to as the stimulus “trigger feature” for this class of cells (Barlow et al. 1964). The idea of a trigger feature is consistent with the findings that these cells respond in a directionally selective (DS) manner to moving stimuli independently of many stimulus parameters (dimensions), such as sign and amount of contrast, spatial configuration, spatial frequency, speed, and motion extent (Grzywacz and Amthor 2007). This robust discrimination is mediated by a number of mechanisms about which a great deal is already known (Amthor and Grzywacz 1991, 1993; Ariel and Daw 1982; Baccus et al. 2008; Barlow and Levick 1965; Caldwell et al. 1978; Grzywacz et al. 1997, 1998a,b; Kittila and Massey 1997; Taylor and Vaney 2002; Taylor et al. 2000; Poggio and Reichardt 1973; Schachter et al. 2010; Wyatt and Daw 1975).

However, the concept of directionality as a trigger feature requires further elaboration because some characteristics of On-Off DS RGCs seem to impede their signaling of the precise direction of motion. First, stimulus dimensions other than

direction also affect responses of these cells. A first-order measure of response magnitude, the number of spikes elicited by a moving stimulus, depends on the contrast, speed, and spatial frequency as well. Second, these cells respond to a broad range of directions, with the response magnitude falling off monotonically from the preferred direction in a gradual manner, and, for instance, they produce responses to directions 90° from the preferred which are typically between 25% (Levick et al. 1969) to 50% (Barlow et al. 1964) of the maximum, much larger than in DS cells in the lateral geniculate nucleus (Levick et al. 1969). Therefore, despite the precise axial directional discrimination of On-Off DS RGCs, the response of a single cell is ambiguous about motion direction, as it cannot distinguish, at least by first-order response magnitude, a nonoptimal contrast stimulus moving close to the preferred direction from an optimal contrast stimulus that is farther from the preferred direction. Consequently, this raises a question about the feasibility of extracting precise information on the stimulus direction from responses of On-Off DS RGCs.

A plausible approach to de-confound stimulus parameters is population coding (Pouget et al. 2000). There is some evidence suggesting that On-Off DS RGCs may implement such a coding scheme with respect to direction. First, the preferred directions of these cells are not uniformly distributed, but are arranged in four clusters, roughly corresponding to the anterior, posterior, superior, and inferior motion in the field of view (Oyster 1968; Oyster and Barlow 1967). Second, each of the four orthogonally tuned cell subclasses tiles the retina precisely (Amthor and Oyster 1995). Consequently, every point in the field of view is projected onto the receptive fields of exactly four On-Off DS RGCs, each preferring a different cardinal direction. If all the stimulus parameters

other than direction affected a quartet of cells identically, a higher visual center could filter out the effects of those parameters by comparing the ratios of these cells' outputs and thus more precisely estimate the direction (van Hateren 1990). However, such an approach would require fulfillment of two, among several other, assumptions: 1) the effects of the nondirectional parameters should be separable from the effect of direction, and 2) the effects of the nondirectional parameters should be the same for all the cells in a population. To address these problems, variation in responses of On-Off DS RGCs across multiple parameters must be determined.

In this study, we pursued these problems by asking the following questions: 1) how does response vary along each stimulus dimension; 2) do the different dimensions affect cell responses independently, or do interactions between them exist; and 3) does the entire population of On-Off DS RGCs in a rabbit retina behave similarly with respect to the first two questions? Such issues have been considered previously with respect to coding strategies of visual cortical cells (Stern et al. 1993). Here we focused on three parameters of a moving stimulus: direction, speed, and luminance.

In sensory neurons, the standard method for assessment of a neuron's response characteristics to a particular stimulus dimension is the neuronal tuning curve, which is a mapping between the stimulus parameter under study and the mean firing rate of the neuron (Dayan and Abbott 2005); thus it provides a first-order description of cell responses as a function of the parameter value. Other studies (Barlow et al. 1964) have shown that On-Off DS RGCs are broadly direction tuned with responses about half maximal to directions up to 90° from the preferred. It has also been determined that On-Off DS RGCs are broadly speed tuned and maintain directional selectivity across more

than two orders of magnitude of speed, from a few tenths of a degree per second to at least 50°/s (Grzywacz and Amthor 2007). In the same study, speed tuning curves for the preferred and null directions were found to be nonmonotonic: increasing for slow speeds, exhibiting a peak around 30°/s, and decreasing for faster speeds. In another study, in which total spikes per sweep was measured rather than mean firing rate, it was found that response decreases as speed increases for the whole range of speeds studied (Wyatt and Daw 1975). The range of speeds investigated was similar in the two studies. On-Off DS RGCs have also been shown to be broadly tuned for contrast, maintaining directional selectivity over the entire range of contrasts to which they respond, even at contrasts of a few percent (Grzywacz and Amthor 2007). Contrast tuning curves for the preferred and null directions determined in that study were found to be nonmonotonic in the same rise-then-fall fashion as speed tuning curves, consistent with an earlier study in which spike count rather than mean firing rate was the response measure (Merwine et al. 1998).

To study the effects of direction, speed, and luminance on the responses of On-Off DS RGCs, we developed a model based on the tuning curves for these three parameters, but rather than the mean firing rate we used the mean spike counts. Our model was therefore constrained to first-order measure of responses, namely the mean number of spikes evoked by a particular stimulus. We found that direction, speed, and luminance had nonlinear characteristics, and we quantified these. In addition, for each cell the general shapes of direction, speed, and luminance tuning curves were independent from the other two parameters, which affected the tuning curve only by a scale factor. Moreover, the speed and luminance tuning curves appeared to be very similar across different cells. Consequently, we found that a simple multiplicatively

separable model employing a Gaussian function to approximate the direction tuning curve, a power function to approximate the speed tuning curve, and an exponential rise function to approximate the luminance tuning curve closely accounted for the mean spike counts for most combinations of stimulus parameter values. Some preliminary results of this study have been previously reported in abstract form (Nowak et al. 2009).

METHODS

All experimental procedures were approved by the University of Alabama at Birmingham Institutional Animal Care and Use Committee (the University of Alabama at Birmingham is accredited by the American Association for Accreditation of Laboratory Animal Care). Retina preparations and electrophysiology methods were similar to those reported by Risner et al. (2010).

Retina Preparation

Small weight New Zealand albino rabbits (1.6–4.2 kg) of both sexes were dark adapted and anesthetized initially by intraperitoneal injections of urethane (2 g/kg; Sigma-Aldrich, St. Louis, MO), followed by administration of Nembutal (Ovation Pharmaceuticals, Lake Forest, IL) through the marginal ear vein until no change in heart rate and no reflexive movement resulting from a pinch to the paw was observed. Under dim red light, the eye was enucleated and the animal was euthanized by an intravenous injection of 1 ml Fatal Plus (Vortech Pharmaceuticals, Dearborn, MI). The eye was hemisected in ice-cold oxygenated bicarbonate-buffered (95% O₂ and 5% CO₂) Ames medium (Sigma-Aldrich, St. Louis, MO), and the lens and vitreous were removed. The remaining eyecup was bisected along the line crossing the optic disc and orthogonal to the fiber band. One of the halves was mounted on a domed chamber where it was superfused with heated (33–35°C) oxygenated bicarbonate-buffered Ames medium (~3.5 ml/min). Ganglion cell somas were visualized using Azure B (Sigma-Aldrich)

solution, a few drops of which were added to the superfusate flowing over the retina (Amthor et al. 2002).

Cell Selection and Categorization

It is known that On-Off DS RGCs in rabbits occur in four broadly tuned directions (Oyster and Barlow 1967), and there is evidence that different directions have different distributions of cholinergic receptor subtypes (Strang et al. 2007). It is also known that the receptive fields of these cells are larger at higher eccentricities than centrally (Levick 1967). In this study, On-Off DS RGCs were recorded from both inferior and superior retina at various eccentricities but mostly just below the visual streak, and the location in the retina and the preferred direction of each recorded cell was noted. However, our sample size was too small to investigate whether any properties related to directional selectivity varied systematically as a function of location or particular preferred direction. Thus our analyses of On-Off DS RGCs were lumped together with respect to particular preferred direction and eccentricity.

Visual Stimuli and Receptive Field Mapping

Stimuli were displayed on a standard 15-inch color CRT monitor (model SyncMaster 15GLi, Samsung, Ridgefield Park, NJ) with 640×480 resolution and 100-Hz refresh rate. The monitor's nonlinear relationship between its luminance and applied grayscale value was measured using a photometer (model LS-110; Minolta). The displayed image was reflected by a mirror that projected it through the epiillumination pathway obtained by removal of the fluorescence lamp housing from a microscope

(model Optiphot-2; Nikon), and having passed a $\times 2$ eye piece followed by a $\times 4$ objective, it was focused on the retina. The aperture of the optical system was 13 mm, and the overall demagnification factor was ~ 59 . The display of the stimuli on the monitor was driven by a custom-developed application DataAcquirer II/AIN (Amthor Laboratory, University of Alabama at Birmingham) running on a personal computer under Microsoft Windows XP Professional operating system (Microsoft, Redmond, WA). During manual receptive field mapping, the stimulus consisted of one small white rectangle flashed or jittered repeatedly on a dark background at different locations. For subsequent data collection, a bar moving perpendicular to its long side was used, with the length of this side being equal to the diameter of the receptive field center. Depending on the experimental protocol, the bar was swept in a number of directions with all the other parameters held constant, or its speed or luminance was varied, either separately or in combination. Bar speed was measured in millimeters per second on the retina, but it was also converted to degrees per second using the retinal magnification factor of $0.173 \text{ mm}/^\circ$ calculated for a rabbit schematic eye by Hughes (1972). In experiments with constant speed, the speed was 2.84 mm/s ($16.42^\circ/\text{s}$), whereas in experiments with variable speeds, five speeds varying between 0.71 mm/s ($4.10^\circ/\text{s}$) and 11.36 mm/s ($65.66^\circ/\text{s}$) were used. Light intensity was reported in terms of luminance, but since luminance is a measure specific to the human observer and not to the retina preparation under the optical system used, the corresponding retina irradiance was also determined. For this purpose, the relationship between the applied grayscale value and the retina irradiance was measured using a light detector (model SED 033/F/W; International Light, Newburyport, MA) connected to a radiometer (model IL 1700; International Light). The readings of the

radiometer were subsequently corrected to account for the fact that the stimulating light did not cover the whole area of the integrating sphere. In experiments with constant luminance level, the bar luminance was 57.58 cd/m^2 (irradiance: $9.73 \text{ } \mu\text{W/cm}^2$) and the background was dark (luminance: 0 cd/m^2 and irradiance: $0.57 \text{ } \mu\text{W/cm}^2$). In experiments with variable luminance levels, five luminance levels varying between the value slightly above the cell threshold determined earlier (the lowest value across all cells was 1.03 cd/m^2 , irradiance: $0.73 \text{ } \mu\text{W/cm}^2$) and 57.58 cd/m^2 were used for the bar, while the background was also kept dark. In experiments involving positive and negative contrasts, three positive and three negative contrasts were used, and the background was mid-gray with the luminance of 28.62 cd/m^2 (irradiance: $5.09 \text{ } \mu\text{W/cm}^2$). The contrasts were calculated as Weber contrasts from the formula $(L_S - L_B)/L_B$, where L_S denotes the stimulus luminance and L_B denotes the background luminance, measured in candelas per meters squared.

Data Recording and Analysis

Extracellular recordings from single cells were obtained using a single carbon-fiber tipped, copper wire in-glass electrode plated with silver chloride (Amthor et al. 2003; Armstrong-James and Millar 1979). The signal was amplified (A-M Systems, Sequim, WA), filtered with a custom-made learning filter to remove 60-Hz noise, thresholded with a custom-made Schmitt trigger, and digitized at a 1-kHz sampling rate using PCI-DAS1002 acquisition board (Measurement Computing, Norton, MA). Action potentials were verified to stem from a single cell by observation on an oscilloscope (Hitachi) and by listening to the audio output. On-line spike extraction was performed by

the DataAcquirer II/AIN application and the resulting spike times were stored to the nearest millisecond on the hard disk for further off-line analyses. Each recording comprised 35 trials in each of which unique conditions (particular combinations of direction, speed, and luminance level) were arranged in a shuffled random order. The collected data were subsequently analyzed off-line using routines written in MATLAB 7.7 (MathWorks, Natick, MA).

Assessment of Directional Selectivity

Directional selectivity of each cell was quantified off-line using the direction selectivity index proposed by Taylor and Vaney (2002):

$$D = \left| \frac{\sum \vec{d}_i}{\sum r_i} \right|,$$

where D represents the direction selectivity index, the summations are performed over all the tested directions, and each d_i is a vector having the same direction as the corresponding stimulus and the length r_i equal to the mean number of spikes elicited by that stimulus. This index ranges from 0, when the mean spike counts are equal in all tested directions, to 1, when a nonzero spike count is obtained only for one direction. Consequently, larger index values indicate stronger directional selectivity.

Fitting of Tuning Curves

Direction, speed, and luminance tuning curves were fitted off-line with various functions using the MATLAB Optimization Toolbox (Version 4.1). The fitting procedure involved a nonlinear least-squares method based on trust-region reflective Newton

algorithm (Optimization Toolbox User's Guide 2008). To assess the robustness of the fits, 95% confidence intervals were computed using MATLAB Statistics Toolbox (Version 7.0). The goodness of fit of different functions was compared by means of adjusted coefficient of determination (adjusted R^2), which was preferred over coefficient of determination (R^2) because of unequal number of the fitted parameters in those functions. Details of the fitting are given in the Appendix.

Similarity Index

Depending on the experimental protocol, various direction, speed, luminance, or contrast tuning curves were obtained for a single cell at different stimulus conditions. Within each tuning category, the similarity of the shapes of those tuning curves was quantified off-line using a similarity index. This index was similar to that introduced by Rapela et al. (2010) except for two differences: it was based on the median rather than the mean as the measure of central tendency and on the Kendall's tau rank correlation coefficient rather than the Pearson product-moment correlation coefficient as the measure of correlation. This modification made it robust against outliers, possibly related to the weakest stimuli. The index was computed in three steps: first, the tuning curves were normalized with respect to their peaks, then the median normalized tuning curve for the cell was determined, and finally the Kendall's tau rank correlation coefficient between the data constituting that median curve and the data corresponding to all the normalized tuning curves was computed yielding the index value. As shown by Rapela et al. (2010), this type of index gives the upper bound of how well a curve can be predicted from the others. Since it is a correlation index, its value ranges from 0, when the curves are

statistically unrelated (which would happen, for example, if they were generated by noise), to 1, when the curves are identical, meaning perfect similarity, or, in the terminology adopted by Rapela et al. (2010), a perfect ability to predict a curve from the others. This index, owing to its statistical nature, also provides a corresponding P value that represents the probability of obtaining a particular value solely by chance, when in fact there is no association among the curves.

RESULTS

We report here the results from several experimental protocols in which a total of 26 On-Off DS RGCs were recorded from 24 rabbit retinas at various eccentricities. Responses of single cells were measured as mean spike counts obtained from averaging the total number of spikes over 35 trials.

Direction Tuning Curves

General characteristics of direction tuning curves. On-Off DS RGCs respond asymmetrically to a stimulus moving in different directions, producing the strongest response when the stimulus is moving in the preferred direction, the weakest response when it is moving in the null direction, and intermediate responses when it is moving in intermediate directions (Barlow et al. 1964). Therefore, their direction tuning curves are unimodal with the peak at the preferred direction and fall gradually in both directions from that preferred direction toward the null direction, at which they reach the minimum. Here, we investigated direction tuning curves of all 26 On-Off DS RGCs with more precision than reported previously in the literature, using 32 directions separated by $\sim 11.25^\circ$ rather than the typical 8 or 16 directions. We swept a bright bar (of luminance 57.58 cd/m^2) on a dark background at a constant speed (2.84 mm/s as measured on the retina, equivalent to $16.42^\circ/\text{s}$) across the receptive field. For each cell, we first assessed its directional selectivity using the direction selectivity index proposed by Taylor and Vaney (2002). We found the indexes to vary between 0.25 and 0.68, with the mean of

0.49 and the SD of 0.11. The latter two values appear similar to those reported by Taylor and Vaney (2002) (mean = 0.57; SD = 0.08) and Zeck and Masland (2007) (mean = 0.58; SD = 0.10), although our mean value is slightly lower.

We next examined the shapes of the direction tuning curves. A polar plot of a representative direction tuning curve obtained from a typical cell is shown in Fig. 1A. Our results confirmed previous findings that direction tuning curves fall off in both hemiplanes from the preferred direction in a generally monotonic and symmetrical manner (Barlow et al. 1964; Oyster 1968). This is demonstrated in Fig. 1B, which replots the data from Fig. 1A in Cartesian coordinates with additional small dots representing spike counts in individual trials. Even though the individual trials exhibited some considerable variability, in a number of cells such as this one, there was effectively no overlap between the responses near the preferred and near the null directions.

We also examined the widths of the direction tuning curves. For each cell, we fitted the mean spike counts with a Gaussian function (1 of the 3 fitted functions used during subsequent functional approximation of direction tuning curves, as described later) and obtained an estimate of the direction tuning width as the half width at half maximum. Figure 1C shows a histogram of these estimates for all the 26 cells. Our results confirmed that On-Off DS RGCs are broadly direction tuned (Barlow et al. 1964; Levick et al. 1969). Specifically, we found that although there was some variability in direction tuning widths as they ranged between $\sim 38^\circ$ (resulting in more elliptical-like tuning curves) and 106° (resulting in more cardioid-like tuning curves), the tuning was generally broad, with the median tuning width of 75.5° . We noted that the shape of the histogram shown in Fig. 1C strongly indicated that the direction tuning widths could stem

from a normal distribution. To verify this hypothesis, we compared the actual distribution of the direction tuning widths with a theoretical distribution being an appropriately scaled normal distribution with the same parameters as those calculated from the data (mean = 76.6° ; SD = 17.91°). As demonstrated in Fig. 1C, a curve representing the theoretical distribution, when overlaid upon the histogram, matched it apparently well. Fig. 1D, in turn, shows a quantile-quantile plot in which the quantiles determined by the actual direction tuning widths are plotted against the corresponding quantiles from the theoretical distribution. In general, the points follow closely the diagonal, indicating that the two distributions are similar, which provides further evidence supporting normality of the distribution of the direction tuning widths. Another hypothesis that we considered was whether direction tuning width is related to the overall excitability of the cell, possibly reflecting the cell health condition. For this purpose, for each of the 26 cells we compared its direction tuning width with the corresponding total of the mean spike counts that was the sum over the 32 tested directions. Likewise, we compared the direction tuning width with the cell spontaneous activity represented by the mean spike counts for no-stimulus (blank) condition. In both cases we did not find any correlation. Figure 1E shows a plot of the total mean spike counts for each cell vs. the direction tuning width. Apparently, the points are randomly scattered, indicating no association, which is confirmed by a very small Pearson product-moment correlation coefficient ($r = 0.12$; $P = 0.56$). A similar plot of the mean spike counts for no-stimulus (blank) condition vs. the direction tuning width is shown in Fig. 1F. The points are also randomly scattered, yielding equally small Pearson product-moment correlation coefficient ($r = -0.07$; $P = 0.72$).

Functional approximation of direction tuning curves. We investigated whether the direction tuning curve can be approximated by some simple functions through fitting the relationship between the stimulus direction and the mean spike counts. We chose three functions with a small number of free parameters: mirror-symmetric Archimedes' spiral (Eq. 2 in Appendix), cosine (Eq. 3), and Gaussian (Eq. 4). The mirror-symmetric Archimedes' spiral was a concatenation of two standard Archimedes' spirals, each confined to one hemi-plane from the preferred direction, as shown in Fig. 2A. This function was selected because it makes two assumptions, which might simplify decoding: 1) the response magnitude is symmetric about the preferred-null direction axis, and 2) in each hemi-plane the response magnitude declines linearly away from the preferred direction. The other two nonlinear functions were selected as they are widely used for fitting neuronal tuning curves (Dayan and Abbott 2005). The cosine function is not as simple as the mirror-symmetric Archimedes' spiral, as it is quadratic in the neighborhood of the peak and linear on the flanks, but it has the advantage of being smooth at the peak. Moreover, a quartet of cosine functions allows representation of the positive projections of direction onto four axes. The Gaussian function, like cosine, is smooth at the peak, and also offers an additional degree of freedom governing its width. In the case of this function, we implemented extra terms to ensure mirror symmetry in both hemi-planes from the preferred direction (see Appendix). A typical fit of the mirror-symmetric Archimedes' spiral, using the data points producing the same direction tuning curve as depicted in Fig. 1, A and B, is shown in Fig. 2B, while Fig. 2, C and D, shows the corresponding fits of the cosine and Gaussian functions, respectively. We found that generally the data points along the slopes were fitted closely by all of the three functions,

but in the regions immediate to the preferred and null directions, in which the direction tuning curves were rather flat, the mirror-symmetric Archimedes' spiral could not follow the data points precisely, as opposed to the two nonlinear functions. This failure of the mirror-symmetric Archimedes' spiral was due to its piecewise linear nature resulting in its pointed shape in these regions. Most commonly, the closest fit was offered by the Gaussian function owing to the additional parameter governing its width. This additional flexibility presented an advantage over the other two functions for two reasons. First, the tuning widths expressed in terms of the half width at half maximum of both the mirror-symmetric Archimedes' spiral and the cosine functions were fixed at 90° , whereas the respective median direction tuning width for all the 26 cells proved to be 75.5° (as described earlier), which means that both of the functions were on average too broad. Second, the width parameter enabled the Gaussian function to adjust even more precisely depending on the individual tuning widths, which could be slightly broader or narrower than the average. Our observations were confirmed when we assessed the goodness of fit of the three functions for all the 26 cells by means of an adjusted coefficient of determination (adjusted R^2), the spread of which is shown in Fig. 2E in the form of a box plot. As expected, the Gaussian function provided the best fit, although the goodness of fit of all the three functions was very high and comparable, with the median values of 0.92, 0.94, and 0.97, for the mirror-symmetric Archimedes' spiral, cosine, and Gaussian functions, respectively. Moreover, the interquartile range of the coefficients (depicted as the box height in Fig. 2E) was substantially smaller for the Gaussian function compared with the other two. Even though this function required one extra parameter to be fitted, the additional degree of freedom seemed justified since the adjusted R^2 , which penalizes

extra parameters, still had the highest value and the smallest variation for the Gaussian function.

Invariance of direction tuning curves to other stimulus parameters. We next investigated how different stimulus parameters affect the shape of the direction tuning curve. First, we examined the effect of speed. Here, we varied speed and direction systematically, sweeping a bright bar (of luminance 57.58 cd/m^2) on a dark background in 16 directions separated by $\sim 22.5^\circ$ at five speeds across the receptive field. Other stimulus parameters except direction and speed were held constant. The data came from 10 cells from 10 different retinas. The results were consistent for nine cells, whereas one cell was found to be anomalous (as its responses were sluggish and not equally DS at all speeds), and thus it was omitted from the analyses. Figure 3A shows a Cartesian plot of the direction tuning curves obtained for the various speeds from the cell that yielded the least noisy data. Generally, as the speed increased, the mean number of spikes decreased, and this outcome was independent of direction (except for the null direction, for which the number of spikes was almost equal at all the speeds). Figure 3B shows the same direction tuning curves normalized with respect to the peak mean spike count for each speed. The normalization resulted in all the curves reducing to the same generic curve, which suggested that the effect of speed on the direction tuning curve can be represented by a multiplicative scale factor. For some cells, this robust normalization failed somewhat only at the fastest speed, which elicited poor responses for most directions away from the preferred, producing the respective normalized direction tuning curve slightly shifted or having a slightly different width compared with the other normalized curves. To assess the extent to which the direction tuning curves for different speeds normalized to one

generic curve in a given cell, we calculated a similarity index (see Methods). Figure 3C shows a histogram of these similarity indexes quantified for all the nine analyzed cells. We found the similarity to be high, with the minimum correlation equal to 0.71, the maximum correlation equal to 0.90, and the median correlation equal to 0.85. All the corresponding P values were below 0.0001.

We also examined the effect of luminance on the direction tuning curve. Here, luminance and direction were varied systematically, using a bright bar at five luminance levels against a dark background, and sweeping it in 16 directions separated by $\sim 22.5^\circ$ at a constant speed (2.84 mm/s as measured on the retina, equivalent to $16.42^\circ/\text{s}$) across the receptive field. Other stimulus parameters except direction and luminance were held constant. The data came from nine cells from nine different retinas, but the results were consistent for eight cells. One cell was found to yield rather anomalous results, and thus it was omitted from the analyses (the same cell that was anomalous when speed was varied). Figure 3D shows a Cartesian plot of the direction tuning curves obtained for the various luminance levels from one of the cells that produced the least noisy data. Generally, as the luminance increased, the mean number of spikes also increased, and this outcome was independent of direction (again except for the null direction, for which the number of spikes was almost equal at all the luminance levels). It is worth pointing out that the ~ 40 -fold variation of luminance in the plot shown in Fig. 3D is reduced to an ~ 2 -fold variation in mean spike count, which constitutes a 20-fold compression. In Fig. 3E, the same direction tuning curves were normalized with respect to the peak mean spike count for each luminance level. As in the case of speed variation, the normalization mapped all the curves onto the same generic curve, which indicated that the effect of

luminance on the direction tuning curve can also be represented by a multiplicative scale factor. This mapping, for some cells, failed somewhat at the lowest luminance level, with the result that the respective normalized direction tuning curve was slightly shifted or changed in width compared with the other normalized curves. As before, we applied the similarity index to each cell to assess the extent to which the direction tuning curves for different luminance levels normalized to one generic curve. Figure 3F shows a histogram of the similarity indexes quantified for all the eight analyzed cells. Again, we found the similarity to be high, with the minimum correlation being 0.75, the maximum correlation being 0.91, and the median correlation being 0.88, and with all the corresponding P values being below 0.0001.

We also examined the effect of covariation of speed and luminance on the direction tuning curve. Here, we used eight directions separated by $\sim 45^\circ$ and all combinations of three speeds and three luminance levels for sweeping a bright bar across the receptive field. The data came from three cells from three different retinas. A Cartesian plot of the direction tuning curves obtained for all the nine combinations of speeds and luminance levels from the cell that yielded the least noisy data is shown in Fig. 3G. Generally, in accord with our previous findings, the mean number of spikes increased as the speed decreased or as the luminance increased; thus the strongest parameter combination was that of the slowest speed and the highest luminance level, whereas the weakest combination comprised the fastest speed and the lowest luminance level. However, at least for those parameter values that we tested, we found that speed contributed a more profound effect on cell response than luminance. As before, we normalized the direction tuning curves with respect to each one's peak mean spike count.

Figure 3H shows the normalized versions of the curves depicted in Fig. 3G. Following normalization, all of the curves, except for that obtained for the weakest parameter combination, were mapped onto the same generic curve. The weakest combination comprised a special case as it yielded cell activity not different than the spontaneous activity, which resulted in the shape of the corresponding direction tuning curve being extremely dependent on random noise. Despite this exception, the results indicated that the combined effect of both speed and luminance on the direction tuning curve can still be represented by a multiplicative scale factor. Using the similarity index, we assessed for each cell the extent to which the direction tuning curves for different combinations of speeds and luminance levels normalized to one generic curve. Figure 3I shows a histogram of similarity indexes quantified for all the three cells. The similarity was still high, with the minimum correlation of 0.69, the maximum correlation of 0.79, and the median correlation of 0.72, and with all the corresponding $P < 0.0001$. Although these index values were slightly smaller than those in the previous experiments, this reduction was mostly caused by the weakest parameter combination, not yielding any significant responses. When this combination was omitted from computations, the correlations were on average 0.09 higher, with the minimum correlation increased to 0.78, the maximum correlation increased to 0.86, and the median correlation increased to 0.82.

Speed Tuning Curves

General characteristics and invariance of speed tuning curves. The mean firing rates of On-Off DS RGCs for the preferred and null directions have been shown to depend on the stimulus speed in a nonmonotonic fashion: they increase for slow speeds,

exhibit a peak around 30°/s, and decrease for faster speeds (Grzywacz and Amthor 2007). However, it has also been shown that, in the preferred direction, the spike count (integral of the spike rate) decreases monotonically with speed (Wyatt and Daw 1975). This is possibly because at lower speeds a longer time on receptive field is not offset by a lower firing rate. Here, we investigated speed tuning curves more thoroughly than reported in the literature, employing more directions than just the preferred and null ones. We used the same data from the nine cells that were analyzed during the investigation of direction tuning curves at five different speeds (as described earlier). This time we plotted the mean spike count vs. speed for eight almost equidistant directions, including the preferred and the null directions. A plot of such speed tuning curves from the cell that yielded the least noisy data is shown in Fig. 4*A*. Generally, as the speed increased, the mean number of spikes decreased, but the relationship appeared highly nonlinear: at the slow speeds a rapid fall occurred, which flattened at the faster speeds. We found these results consistent with those reported by Wyatt and Daw (1975). We also observed that, independent of direction, the speed tuning curves were similar in shape, although they differed in maximum and minimum values. Figure 4*B* shows the same speed tuning curves normalized with respect to the peak mean spike count for each direction. The normalization resulted in all the curves reducing to the same generic curve, suggesting that the effect of direction can be represented by a multiplicative scale factor. To further assess the extent to which the speed tuning curves for different directions normalized to one generic curve, we used the similarity index in the same manner as for direction tuning curves. Unlike in Fig. 4, *A* and *B*, which shows speed tuning curves for only eight directions, the similarity index was computed for each cell utilizing the speed tuning

curves for all the 16 directions available from the data. Figure 4C shows a histogram of these similarity indexes quantified for all the nine analyzed cells. We found that the similarity was high, with the minimum correlation equal to 0.62, the maximum correlation equal to 0.86, and the median correlation equal to 0.74, and with all the corresponding P values being below 0.0001.

We also examined whether the characteristics of speed tuning curves are individual to each cell or rather shared across various cells. For this purpose, we determined the speed tuning curves for the preferred direction for each of the nine analyzed cells. However, due to different excitability in those cells (possibly because of different health conditions of the retinas as well as other factors), the speed tuning curves varied considerably in magnitude. Therefore, to draw comparisons, we normalized them with respect to each one's peak mean spike count. The normalized curves are shown in Fig. 4D. It is apparent that they overlap considerably, which is consistent with the notion of a universal speed tuning in these cells.

Functional approximation of speed tuning curves. We investigated whether the speed tuning curve can be approximated in a functional form, and to this end we attempted to fit the normalized speed tuning curves obtained for the preferred directions from all the nine analyzed cells with two functions that in general resembled their shape: power (Eq. 5 in Appendix) and exponential decay (Eq. 6). Figure 5A shows the fit of the power function, and Fig. 5B shows the fit of the exponential decay. The power function yielded the following values of the fitted parameters: gain = 0.77 [95% CI = (0.70, 0.85)], offset = 0.03 [95% CI = (-0.03, 0.10)], and exponent = -0.65 [95% CI = (-0.75, -0.56)]. The exponential decay, in turn, produced the following parameters: gain = 1.24 [95% CI

= (1.15, 1.33)], offset = 0.23 [95% CI = (0.20, 0.25)], and decay constant = 0.69 [95% CI = (0.61, 0.78)]. Both functions fitted the curves closely, which was confirmed by assessment of the goodness of fit measured as the adjusted R^2 : it was 0.99 for the power function and 0.98 for the exponential decay, respectively. It is worth pointing out that the tuning curves are not well characterized by the stimulus time on receptive field, which would correspond to an exponent of -1 for the power function. As the mean spike count falls more slowly than the time on receptive field, these curve fits imply that, over the limited range of the speeds tested, the spike rate increases with speed.

Luminance Tuning Curves

General characteristics and invariance of luminance tuning curves. The responses of On-Off DS RGCs for the preferred and null directions have been shown to depend nonmonotonically on the stimulus contrast: they increase at low contrasts and, after reaching a peak, decrease at high contrasts, both when the mean firing rate (Grzywacz and Amthor 2007) and the mean spike count (Merwine et al. 1998) are considered. Here, we investigated a closely related cell characteristic, namely luminance tuning curves, employing more directions than just the preferred and null ones. We used the same data from the eight cells that were analyzed during the investigation of direction tuning curves at five different luminance levels (as described earlier). This time we plotted the mean spike count vs. luminance for eight almost equidistant directions, including the preferred and the null directions. Figure 6A shows a plot of such luminance tuning curves from the cell that yielded the least noisy data. Generally, as the luminance increased, the mean number of spikes also increased, but in a highly nonlinear fashion: at

the low luminance levels it exhibited a rapid rise followed by a plateau indicating saturation at the high luminance levels. Contrary to the results reported by Merwine et al. (1998) for contrast, we did not observe a fall in response at high luminance levels, possibly because the luminance levels that we tested were not high enough to elicit this effect. As in the case of speed, we found that the luminance tuning curves were similar in shape independent of direction, although they differed in maximum and minimum values. Figure 6B shows the same luminance tuning curves normalized with respect to the peak mean spike count for each direction. As with speed, the normalization reduced all the curves to the same generic curve, suggesting that the effect of direction can be represented by a multiplicative scale factor. In the same manner as before, we applied the similarity index to each cell to assess the extent to which the luminance tuning curves for different directions normalized to one generic curve, utilizing for its computation the luminance tuning curves for all the 16 directions available from the data. Figure 6C shows a histogram of the similarity indexes quantified for all the eight analyzed cells. We found that the similarity was generally high, with the median correlation of 0.53 and the maximum correlation of 0.80, except for one outlier that was equal to 0.04 (the second smallest value was 0.42). All the corresponding P values apart from that associated with the outlier ($P = 0.63$) were below 0.0001. The outlier stemmed from the fact that for this particular cell the luminance tuning curves were very noisy and often not monotonic (surprisingly, the similarity index for the corresponding direction tuning curves was as high as 0.75).

We examined whether the characteristics of luminance tuning curves are individual to each cell or instead common across various cells, and to this end we

determined the luminance tuning curves for the preferred direction for each of the eight analyzed cells. As in the case of speed, we found them to vary considerably in magnitude due to different excitability in those cells, and likewise, we normalized them with respect to each one's peak mean spike count. The normalized curves are shown in Fig. 6D, but there is one significant difference from the corresponding plot of speed tuning curves. The speeds at which the responses were measured were exactly the same for all the cells, whereas the luminance levels, apart from the highest one, mostly differed among the cells due to different luminance thresholds and the resultant different partitioning of the available range. Despite this dissimilarity, it appears that all of the normalized luminance tuning curves substantially overlap for all the luminance levels except for the lowest ones, which were close to individual cell thresholds.

Functional approximation of luminance tuning curves. We investigated whether the luminance tuning curve can be approximated in a functional form by attempting to fit the normalized luminance tuning curves obtained for the preferred directions from all the eight analyzed cells with three functions that generally resembled their shape: exponential rise (*Eq. 7* in Appendix), rectangular hyperbola (i.e., Michaelis-Menten equation; *Eq. 8*), and logarithmic (*Eq. 9*). Figure 7A shows the fit of the exponential rise, whereas the fit of the rectangular hyperbola and the fit of the logarithmic function are shown in Fig. 7, B and C, respectively. The exponential rise yielded the following values of the fitted parameters: gain = 0.78 [95% CI = (0.68, 0.88)], offset = 0.19 [95% CI = (0.09, 0.30)], and rise constant = 0.11 [95% CI = (0.08, 0.15)]. The rectangular hyperbola produced the following parameters: gain = 0.99 [95% CI = (0.84, 1.13)], offset = 0.09 [95% CI = (-0.07, 0.26)], and rate constant = 5.46 [95% CI = (2.43, 8.48)]. The

logarithmic function delivered the following parameters: gain = 0.21 [95% CI = (0.18, 0.24)] and offset = 0.18 [95% CI = (0.09, 0.27)]. For all these functions we assessed the goodness of fit in the form of the adjusted R^2 , which was 0.88 for both the exponential rise and the rectangular hyperbola, and 0.85 for the logarithmic function, respectively. We found that the fits of all the three functions were good, although at the low luminance levels cells had different thresholds resulting in some scatter of the initial points of the individual luminance tuning curves. We also found that the logarithmic function overestimated the luminance tuning curves at the high luminance levels, because, being an increasing function, it was not able to fit their characteristic saturation.

Response Model

Model development. One important consequence of our finding that the effects of speed and luminance on direction tuning curve could be reduced to multiplicative scale factors, as could the effect of direction on the speed and luminance tuning curves, is that the response measured as the mean spike count is affected by these three stimulus parameters independently, and thus their effects could be multiplicatively separated. Therefore, we attempted to develop a model predicting the mean spike count in On-Off DS RGCs that would be based on a multiplication of three independent functions (*Eq. 1* Appendix): the first one accounting for the effect of direction (direction factor), the second one accounting for the effect of speed (speed factor), and the third one accounting for the effect of luminance (luminance factor). Drawing from our results on fitting of the tuning curves (as described earlier), we chose the Gaussian function to represent the direction factor, the power function to represent the speed factor, and the exponential rise

function to represent the luminance factor. In the light of different cell excitability as well as the known differences in the preferred directions, we assumed in the model that the direction tuning curve should be fitted on an individual cell basis. On the other hand, our findings indicating that the speed and luminance tuning curves could be common to all On-Off DS RGCs allowed us to employ in the model the population fits of the speed and luminance tuning curves. In fact, these fits were obtained for the normalized speed and luminance tuning curves, but this was actually desired from the model perspective, as the model assumed that the direction tuning curve would be fitted using that combination of speed and luminance level which yielded the strongest responses.

Model tests. To test our model, we used the same data from the three cells that were analyzed during the investigation of direction tuning curves at the nine combinations of three different speeds and three different luminance levels (as described earlier). It should be noted that none of these cells were utilized for fitting either the normalized speed tuning curves (shown in Fig. 5) or the normalized luminance tuning curves (shown in Fig. 7). For each of the three cells, we performed the following procedure. First, we fitted the Gaussian function to the direction tuning curve obtained for the slowest speed and the highest luminance level, as this combination produced the strongest responses. Second, for each combination of speed and luminance level, we computed model predictions of the mean spike counts for all eight directions tested, using the fits shown in Figs. 5A and 7A. Finally, we compared those predictions with the actual mean spike counts. Figure 8 shows such a comparison for one of the cells (the same cell as in Fig. 3, *G* and *H*). The results are divided into separate plots for each combination of

speed and luminance levels, each of which contains eight points corresponding to the eight directions. We found that the model was accurate for almost all stimuli.

The only deviation from accuracy occurred for the weakest stimuli. Specifically, for all three cells the model overestimated the mean spike counts for the combination of the fastest speed and the lowest luminance level, doing the same for two cells at the combination of the fastest speed and the intermediate luminance level. As mentioned earlier, the combination of the fastest speed and the lowest luminance level comprised a special case, as it yielded cell activity not different than the spontaneous activity. As shown in Fig. 8, except for this one combination at which the stimulus failed to drive the cell, the correlation coefficients were in the range 0.96–0.99 (0.99 for 5 of the 8 combinations), indicating that the model captured the data very well.

The summarized results of the model tests on all three cells are shown in Fig. 9. Figure 9A shows a comparison between the predicted spike counts vs. the mean spike counts for all the combinations of speeds and luminance levels separately for each cell. To quantify the accuracy of the predictions, for each cell we computed a linear correlation between the predictions and the actual mean spike counts individually for every combination of speeds and luminance levels. The spreads of the Pearson product-moment correlation coefficients are shown in Fig. 9B. We found these coefficients to be generally close to 1 (mean for the 3 cells of the median $r = 0.98$; $P < 0.0001$). For each cell, we also performed a linear regression analysis, again considering each combination of speeds and luminance levels individually. Figure 9C shows the spreads of the slopes of the linear regression, which we found to be generally close to 1 (mean median slope =

1.08). Figure 9D, in turn, shows the spreads of the intercepts of the regression, which were usually close to 0 (mean median intercept = 0.15).

Figures 8 and 9 demonstrate that a multiplicatively separable model in which the speed and luminance factors are based on population fits while the direction factor is fitted on an individual cell basis provides a very good account of the first-order measure of On-Off DS RGC responses over a substantial range of speeds and luminance levels. Consequently, directionality is invariant up to a scale factor determined by the product of speed and luminance factors.

Luminance vs. contrast. Although we developed our model employing luminance rather than contrast, we also examined whether the effect of direction is separable from the effect of contrast. Here, we varied contrast and direction systematically, using a mid-gray background (of luminance 28.62 cd/m^2) and a bar that was either lighter or darker than the background. Three negative and three positive contrasts were employed for the bar, which was swept in 16 directions separated by $\sim 22.5^\circ$ at a constant speed (2.84 mm/s as measured on the retina, equivalent to $16.42^\circ/\text{s}$) across the receptive field. Other stimulus parameters except direction and contrast were held constant. The data came from nine cells from eight different retinas. Figure 10A shows a Cartesian plot of the direction tuning curves obtained for the various contrasts from the cell that produced the least noisy data. Generally, as the absolute contrast increased, the mean number of spikes also increased, and this outcome was independent of direction (except for the null direction, for which the number of spikes was almost equal at all the contrasts). This result is similar to that yielded by luminance variation (see Fig. 3D). Figure 10B shows the same direction tuning curves normalized with respect to the peak mean spike count

for each contrast. As a result of this normalization, all the curves reduced to the same generic curve, which indicated that the effect of contrast on the direction tuning curve can be represented by a multiplicative scale factor just as the effect of luminance can (see Fig. 3E). For each cell, we also assessed the extent to which the direction tuning curves for different contrasts normalized to one generic curve by applying the similarity index. Figure 10C shows a histogram of the similarity indexes quantified for all the nine cells. We found that the similarity was high, with the minimum correlation of 0.54, the maximum correlation of 0.84, and the median correlation of 0.80, and with all the corresponding P values below 0.0001, although we noticed that these index values were slightly smaller than those obtained for luminance variation (see Fig. 3F). Especially, the minimum correlation was comparatively low, but this outcome was explained by the fact that for this particular cell the weakest positive and the weakest negative contrasts yielded activity not different than the spontaneous activity, which resulted in the shapes of the corresponding direction tuning curves being extremely dependent on random noise. When these two contrasts were omitted from computations for this cell, the correlation increased to 0.82.

DISCUSSION

In this study, we quantitatively investigated how three parameters of a moving stimulus, namely its direction, speed, and luminance, affect the mean spike count responses of On-Off DS RGCs in rabbits. We thus addressed in these cells a portion of the encoding problem involving the interactions among the three parameters. This investigation was motivated by the question of whether, given the exquisite preferred-null axial selectivity for direction exhibited by On-Off DS RGCs on the one hand but the general ambiguity of their responses about the stimulus direction on the other, the strategy of encoding stimulus dimensions in these cells may facilitate subsequent direction decoding.

Our main findings were that 1) direction, speed, and luminance tuning curves are each invariant with respect to the other two stimulus parameters (up to a scale factor), and, as a consequence, the effects of these three parameters are multiplicatively separable, and that 2) speed and luminance tuning curves appear to be common across the whole population of On-Off DS RGCs. Moreover, we confirmed previous findings that direction tuning curves of these cells are broad.

Direction Decoding Problem and Population Coding

Van Hateren (1990) indicated that when responses of visual movement detectors also depend on nondirectional stimulus parameters, such as contrast and speed, the output of a single detector does not permit the precise determination of the stimulus direction

because the effects of the nondirectional parameters confound the information on direction. However, a population code in which at least two detectors are used can resolve the ambiguity as direction can be uniquely represented by the ratio of their responses. This is possible when at least two detectors in the population meet the following criteria: 1) each detector has a different preferred direction, and these preferred directions are sufficiently separated from each other (otherwise the ratio of responses may change very little over a range of directions); 2) the detectors have overlapping direction tuning curves, meaning that these curves must be sufficiently broad; 3) the direction tuning curves vary for different directions (because constant functions will not yield a change in their ratio for different directions); 4) responses of the detectors depend in the same manner on the nondirectional stimulus parameters; and 5) the effect of the nondirectional parameters is multiplicatively separable from the effect of direction. A population code subject to the above assumptions presents an additional advantage; namely, it permits isotropic estimates of direction in the presence of noise, that is estimates without systematic errors (unbiased) and with similar random errors (equally accurate) in any direction (van Hateren 1990).

Broad Direction Tuning

In this study, we confirmed previous findings that direction tuning curves of On-Off DS RGCs are broad and appear to be smooth, monotonic, and symmetrical functions of direction away from the preferred direction (Barlow et al. 1964; Levick et al. 1969). Although we found some spread in direction tuning width, the distribution appeared to be normal, meaning that there were no systematic differences across different cells.

Moreover, the tuning widths seemed not to be related to the cell health condition because tuning width did not correlate with overall excitability.

Given that the preferred directions of On-Off DS RGCs cluster in four groups, roughly corresponding to the anterior, posterior, superior, and inferior motion in the field of view (Oyster 1968; Oyster and Barlow 1967), curves with these characteristics appear to meet three of the criteria set forth by van Hateren (1990). First, the four preferred directions are distinct and separated by $\sim 90^\circ$. With the direction tuning width taken into account, this separation is sufficient to avoid constant response ratios. Second, the distribution of the preferred directions and the direction tuning width imply that direction tuning curves belonging to different groups are sufficiently broad to overlap with one another. Finally, the direction tuning curves vary with direction in a well-behaved manner as determined by their shape. Consequently, broad direction tuning of On-Off DS RGCs does not seem an impediment from the perspective of direction coding but, on the contrary, appears as an advantage facilitating population coding of direction in these cells.

Universal Nondirectional Tuning Curves, Separability, and Hypothesis of “Equivalent Contrast” Normalization

Our finding that all the On-Off DS RGCs that we studied shared the same speed and luminance tuning curves accords with another criterion set forth by van Hateren (1990). Since our sample consisted of cells located at various eccentricities in both inferior and superior retina, we may assume that these curves are indeed universal and not just common to cells in a specific region. However, from the perspective of direction

decoding, universal tuning of all the nondirectional stimulus dimensions is not strictly required. Instead, what the criterion implies is that the tuning of every nondirectional parameter should be common within each local population, which, in turn, would allow some variability among different populations, for example, at different retinal locations. This relaxation could affect such stimulus dimensions that may be, for instance, closely related to the receptive field size. This cell characteristic is actually known to vary regionally: the receptive fields are larger in On-Off DS RGCs at higher eccentricities than in those located centrally (Levick 1967); within a given region, however, their sizes appear to be similar. Therefore, although we examined the tuning curves for those two parameters only, we believe that a similar outcome is likely to apply to other nondirectional stimulus dimensions, either in a truly universal or locally restricted manner.

The last criterion set forth by van Hateren (1990) is addressed by another finding of ours, namely that the effects of stimulus direction, speed, and luminance were multiplicatively separable. Again, we examined only these three parameters of a moving stimulus out of the many possible, but we believe that the separability of the effect of direction from the effects of all the other nondirectional parameters not considered in our study also holds true. As before, however, it is important to emphasize that from the perspective of direction decoding it is not necessary for each nondirectional parameter to be completely separable from all the other parameters. What is essential is that the combined effects of all the nondirectional parameters be separable from the sole effect of direction (see later discussion on selectivity of temporal vs. spatial frequencies).

The above findings together with the idea, supported by some previous evidence (Amthor and Oyster 1995; Oyster 1968; Oyster and Barlow 1967), that every point in the field of view is projected onto the receptive fields of exactly four On-Off DS RGCs, each preferring a different cardinal direction, lead us to the following hypothesis of “equivalent contrast” normalization. It states that for a quartet of cells with receptive fields at a given locus all the nondirectional stimulus parameters, such as contrast, speed, or size, can be lumped together into one “equivalent contrast” super-parameter, accounting for their combined effects. Consequently, this “equivalent contrast” super-parameter could be subsequently isolated from the only parameter that is strongly different among such a local population of On-Off DS RGCs, namely their direction preference, which, in turn, would permit extraction of the stimulus direction. This extraction, as proposed by van Hateren (1990), could be achieved by comparing ratios of responses from the four cells in the population or by other straightforward computations.

Luminance vs. Contrast

Although we developed our multiplicatively separable model based on luminance tuning curves rather than contrast tuning curves, we expect that similar results would be obtained when using the latter, for the following reasons. First, our data from the experiments involving positive and negative contrasts show that direction tuning curves normalize to the same generic curve irrespective of the amount or sign of contrast (see Fig. 10), which indicates that the effect of direction is separable from the effect of contrast in the same manner as it is separable from the effect of luminance. Second, On-Off DS RGCs are generally equally responsive and equally DS for light and dark stimuli

(Barlow and Levick 1965; Taylor and Vaney 2002). Third, these cells exhibit similar dendritic ramifications in the inner and outer plexiform layers (Amthor et al. 1984, 1989).

Unlike the mean spike count speed response, which varied over a wide range of speeds, the mean spike count luminance response varied over only a narrow range of luminance values. Consequently, as luminance saturated above some moderate value, it did not contribute to the response magnitude. Luminance thus behaves as a compressive function, and as a result it permits more of the channel capacity to be devoted to motion-related stimulus dimensions. This finding is similar to what is seen in cortical area MT for contrast (Sclar et al. 1990). Indeed, several similarities between the responses of On-Off DS RGCs and MT cells in primates have been observed (Grzywacz and Amthor 2007), and there is also some evidence in primates for a direct projection from lateral geniculate nucleus to area MT, bypassing V1 (Sincich et al. 2004).

We note that, contrary to the results reported by Merwine et al. (1998) for contrast, we did not observe a fall in response magnitude at high luminance levels. This, however, may be explained by the possibility that the luminance levels that we tested were not high enough to elicit this effect.

Other Stimulus Dimensions and Types

If On-Off DS RGCs indeed utilize “equivalent contrast” normalization for coding stimulus direction, it should perform universally across various stimulus dimensions and types. Here we examined only one type of stimulus, namely a bar, and only two nondirectional stimulus parameters, namely speed and luminance. Therefore, the question whether similar results could be obtained for other stimulus parameters, such as size or

shape, as well as other kinds of stimuli, such as gratings, dot, or texture patterns, remains open.

There is some evidence indicating that the answer would be positive. For instance, Grzywacz and Amthor (2007) have shown that directional selectivity of On-Off DS RGCs appears quantitatively similar for both spots and sinewave gratings. However, some other evidence suggests that it may not be so straightforward. Hammond and Smith (1983), for example, have shown in complex cells of cat striate cortex that direction tuning curves may be subject to change depending on the exact stimulus configuration. They have shown that the preferred direction for a bar and for a texture in the same cell may be different, the direction tuning curves for these two stimuli may have different bandwidths, and the shape of the direction tuning curve for texture alone is affected by speed. Some findings suggest that similar phenomena may occur in On-Off DS RGCs. Grzywacz and Amthor (2007) have observed in a proportion of On-Off DS RGCs a splitting of the preferred direction into two “horns” off the original preferred-null axis for sinusoidal gratings at high spatial frequencies. They proposed an explanation that at spatial frequencies higher than optimum a grating oriented off-axis has a projection on the original preferred-null axis at a lower equivalent spatial frequency, closer to the optimum, and thus evokes a stronger response than the same grating oriented on-axis. A similar splitting of direction tuning curves for textures at high speeds has been observed by Hammond and Smith (1983) in their study on cat complex cells, again only in a proportion of cells, but an analogous explanation, although considered, was rejected in that study. Grzywacz and Amthor (2007) have also found the bandwidths of speed tuning of On-Off DS RGCs for a grating and for a spot to be slightly different, the latter being

somewhat broader. Moreover, they reported that responses of On-Off DS RGCs to drifting gratings of varying spatial and temporal frequencies are roughly separable and not oriented along an isospeed contour in spatial frequency vs. temporal frequency contour plots. Those plots indicate that these cells are tuned to a particular spatial frequency irrespective of temporal frequency (see also He and Levick 2000), and hence they are not strictly speed tuned. Consequently, selectivity for speed is not an invariant characteristic of the responses of these cells since the optimum speed changes as a function of stimulus composition. From this perspective, On-Off DS RGCs are similar to other DS cells in the higher visual centers, such as V1, which also show spatiotemporal separability rather than speed invariance (Holub and Morton-Gibson 1981; Ikeda and Wright 1975; Tolhurst and Movshon 1975). Nevertheless, although the optimum speed varies with stimulus composition, this does not preclude the use of “equivalent contrast” normalization to extract direction from a local population of On-Off DS RGCs all experiencing the same complex stimulus.

Another concern regarding a universal performance of the “equivalent contrast” normalization is related to the fact that a single bar that we used as a stimulus is not very representative for natural scenes since natural sensory inputs usually do not consist of isolated simple patterns (Felsen and Dan 2005). Therefore, it would be compelling to confirm the “equivalent contrast” normalization using movies from rabbit’s natural environment. Likewise, we did not consider here an issue concerning complex effects of adaptation and relative motion between local area and background (Chiao and Masland 2003; Ölveczky et al. 2003, 2007), which also should be addressed.

Consequently, the stimulus regimes under which “equivalent contrast” normalization might be valid are still to be thoroughly investigated.

Spike Count as a Measure

In this study, we used mean spike count as the measure of cell responses, but there are other characteristics of responses of On-Off DS RGCs that could conceivably figure in the refinement of coding for direction. This is because different response measures can yield somewhat different tuning profiles, and thus the same response can be simultaneously characterized in more than one dimension, which, in turn, may facilitate coding precision. For instance, Wyatt and Daw (1975) have demonstrated such a change in tuning profile in On-Off DS RGCs for speed examined at the preferred direction by showing that as the total number of spikes decreases monotonically when the stimulus speed increases, at the same time the peak firing rate increases for low speeds, reaches a maximum $\sim 30^\circ/\text{s}$, and then decreases. They concluded that although it was not clear which response measure is better for characterizing cell activity, the peak firing rate is the one that subsequent neurons can analyze in realistically short time intervals. Amthor et al. (2005) have described another example of coding strategy exhibited by On-Off DS RGCs, namely correlated firing. They have found that synchronous spikes among neighboring On-Off DS RGCs carry additional information about moving stimuli extending across receptive fields of these cells, indicating that the cells are responding together to a contour of a common object. Correlated firing for contours in this and other classes of retinal ganglion cells has been further elaborated by Chatterjee et al. (2007). Such coding could conceivably be robust in the cases where our model was weakest, that

is for fast speed or low contrast stimuli near threshold. Lastly, there is evidence that neither total spikes nor firing rate convey all the information about a stimulus that is encoded by ganglion cells (Jacobs et al. 2009).

The limitation of using spike counts is clearly problematic for assessment of speed tuning, for several reasons. First, counting the total spikes produced by the passage of a discrete stimulus effectively means different integration times for different speeds. This problem gets further complicated by the fact that for the same speeds large textured objects yield responses that last longer than those elicited by small objects, meaning that speed becomes confounded with object size in a spike count. Second, reliable inference by the brain on such rapidly changing stimulus parameters as speed requires use of an “instantaneous” firing rate rather than a mean firing rate, as otherwise decoding of those parameters could become corrupted by changes in the visual scene over long periods.

Model Limitations

Although our multiplicatively separable model generally predicted mean spike counts with a remarkable accuracy, it systematically failed for the weakest stimuli (comprising the combinations of the fastest speed and the lowest or the intermediate luminance level), for which it yielded predictions larger than the corresponding data. As a possible solution, we expect that a simple extension of the model employing a low-response threshold-like nonlinearity could improve its performance for such stimuli. This nonlinear stage would follow the current multiplicatively separable stage, the output of which for the weakest stimuli might often be below the threshold. Consequently, the small predictions obtained for these stimuli from the multiplicatively separable stage

would be transformed into even smaller overall predictions, which, in turn, would make the model closer to the data.

Another limitation of our model stems from the fact that it was developed based on neuronal tuning curves, which are derived from responses to the same stimulus averaged over multiple presentations. In the real world, however, the brain does not need repetitions of stimuli to process them but instead operates on their single occurrences. Therefore, if separability of stimulus parameters is to be utilized for direction decoding, it should also be applicable on a single trial basis. This issue is not addressed here, neither is a related problem of noise present in response magnitude over different trials.

Conclusions

Notwithstanding the above considerations, the findings reported here substantiate two important conclusions. First, the precise preferred-null axial discrimination but broad direction tuning otherwise makes sense if On-Off DS RGCs convey information on stimulus direction by means of a population code. Moreover, such an arrangement might offer an additional advantage in terms of minimizing the number of axons in the optic nerve necessary to transmit this information to the higher visual centers in the brain. Direction representation in these centers could then be transformed from fewer broadly tuned On-Off DS RGCs to a larger number of more narrowly tuned DS cells in some combinatorial coding scheme (Osborne et al. 2008). Second, separability of parameter encoding by On-Off DS RGCs would allow the higher visual centers to normalize away the effects of the nondirectional stimulus parameters through comparing ratios of the responses from the cells in a population or by other straightforward computations.

Assuming that such a population comprises a quartet of orthogonally tuned On-Off DS RGCs with overlapping receptive fields, this could give rise to discrimination of many more than the four directions preferred by those cells. This idea is analogical to color perception, where hundreds of colors can be discriminated from just three photoreceptor classes.

Finally, we conclude that these findings add a strong support to the concept that On-Off DS RGCs in rabbits use a population code for signaling direction, which, in turn, would simplify direction decoding by the higher visual centers in the brain.

APPENDIX

General Form of the Model

We investigated a multiplicatively separable model of responses of On-Off DS RGCs in the following form:

$$r = f(d) \cdot g(s) \cdot h(l), \quad (1)$$

where r denotes cell response expressed as mean number of spikes, f denotes function representing the effect of direction d , g stands for function representing the effect of speed s , and h stands for function representing the effect of luminance l .

Direction Fitting

For derivation of the function representing the effect of direction, we fitted direction tuning curves with three functions: mirror-symmetric Archimedes' spiral, cosine, and Gaussian. All these functions depended on a single variable d denoting stimulus direction (measured in deg, $d \in [0, 360)$). The mirror-symmetric Archimedes' spiral function employed three parameters: a – gain, b – offset, d^* – preferred direction, and took the following form:

$$f_s(d) = a \cdot \left| 180 - \|d - d^*\| \right| + b. \quad (2)$$

The cosine function employed the same three parameters: a – gain, b – offset, d^* – preferred direction, and took the following form:

$$f_c(d) = a \cdot \cos\left(\frac{\pi}{180} \cdot (d - d^*)\right) + b. \quad (3)$$

The Gaussian function employed four parameters: a – gain, b – offset, c – tuning width (expressed in the form of SD), d^* – preferred direction, and took the following form:

$$f_G(d) = a \cdot \exp\left(-\frac{(180 - |180 - |d - d^*||)^2}{2c^2}\right) + b. \quad (4)$$

Additional expressions involving absolute values and the number 180 in the formula of the Gaussian function were used to ensure mirror symmetry of this function in both hemiplanes from the preferred direction.

Speed Fitting

For derivation of the function representing the effect of speed, we fitted speed tuning curves with two functions: power and exponential decay. Both functions depended on a single variable s denoting stimulus speed (measured in mm/s on the retina). The power function employed three parameters: a – gain, b – offset, c – exponent, and took the following form:

$$g_p(s) = a \cdot s^c + b. \quad (5)$$

The exponential decay function also employed three parameters: a – gain, b – offset, c – decay constant, and took the following form:

$$g_e(s) = a \cdot \exp(-c \cdot s) + b. \quad (6)$$

Luminance Fitting

For derivation of the function representing the effect of luminance, we fitted luminance tuning curves with three functions: exponential rise, rectangular hyperbola, and logarithmic. All these functions depended on a single variable l denoting stimulus luminance (measured in cd/m^2). The exponential rise function employed three parameters: a – gain, b – offset, c – rise constant, and took the following form:

$$h_e(l) = a \cdot (1 - \exp(-c \cdot l)) + b. \quad (7)$$

The rectangular hyperbola also employed three parameters: a – gain, b – offset, c – rate constant, and took the following form:

$$h_r(l) = a \cdot \frac{l}{c + l} + b. \quad (8)$$

The logarithmic function employed two parameters: a – gain, b – offset, and took the following form:

$$h_l(l) = a \cdot \ln(l + 1) + b. \quad (9)$$

ACKNOWLEDGMENTS

We thank John Tootle for programming assistance and Jordan Renna, Michael Risner, and Kent Keyser for technical assistance and suggestions.

GRANTS

This work was supported by the National Science Foundation Grant IOB 0622318 (to T. J. Gawne), EyeSight Foundation of Alabama Grant FY2005-06-26 (to F. R. Amthor), and National Institutes of Health Grant P30-EY-03039 (University of Alabama at Birmingham Vision Science Research Center Core).

DISCLOSURES

No conflicts of interest, financial or otherwise, are declared by the author(s).

REFERENCES

- Amthor FR, Grzywacz NM. The nonlinearity of the inhibition underlying retinal directional selectivity. *Vis Neurosci* 6: 197-206, 1991.
- Amthor FR, Grzywacz NM. Inhibition in On-Off directionally selective ganglion cells in the rabbit retina. *J Neurophysiol* 69: 2174-2187, 1993.
- Amthor FR, Keyser KT, Dmitrieva NA. Effects of the destruction of starburst cholinergic amacrine cells by the toxin AF64A on rabbit retinal directional selectivity. *Vis Neurosci* 19: 495-509, 2002.
- Amthor FR, Oyster CW. Spatial organization of retinal information about movement detection. *Proc Natl Acad Sci USA* 92: 4002-4005, 1995.
- Amthor FR, Oyster CW, Takahashi ES. Morphology of on-off direction-selective ganglion cells in the rabbit retina. *Brain Res* 298: 187-190, 1984.
- Amthor FR, Takahashi ES, Oyster CW. Morphologies of rabbit retinal ganglion cells with complex receptive fields. *J Comp Neurol* 280: 97-121, 1989.
- Amthor FR, Tootle JS, Grzywacz NM. Stimulus-dependent correlated firing in directionally selective retinal ganglion cells. *Vis Neurosci* 22: 769-787, 2005.
- Amthor FR, Tootle JS, Yildirim A. A new transparent multi-unit recording array system fabricated by in-house laboratory technology. *J Neurosci Methods* 126: 209-219, 2003.
- Ariel M, Daw NW. Pharmacological analysis of directionally sensitive rabbit retinal ganglion cells. *J Physiol* 324: 161-185, 1982.
- Armstrong-James M, Millar J. Carbon fibre microelectrodes. *J Neurosci Methods* 1: 279-287, 1979.
- Baccus SA, Ölveczky BP, Manu M, Meister M. A retinal circuit that computes object motion. *J Neurosci* 28: 6807-6817, 2008.
- Barlow HB, Hill RM. Selective sensitivity to direction of movement in ganglion cells of the rabbit retina. *Science* 139: 412-414, 1963.
- Barlow HB, Hill RM, Levick WR. Retinal ganglion cells responding selectively to direction and speed of image motion in the rabbit. *J Physiol* 173: 377-407, 1964.

- Barlow HB, Levick WR. The mechanism of directionally selective units in the rabbit's retina. *J Physiol* 178: 477-504, 1965.
- Caldwell JH, Daw NW, Wyatt HJ. Effects of picrotoxin and strychnine on rabbit retinal ganglion cells: lateral interactions for cells with more complex receptive fields. *J Physiol* 276: 277-298, 1978.
- Chatterjee S, Merwine DK, Amthor FR, Grzywacz NM. Properties of stimulus-dependent synchrony in retinal ganglion cells. *Vis Neurosci* 24: 827-843, 2007.
- Chiao CC, Masland RH. Contextual tuning of direction-selective retinal ganglion cells. *Nat Neurosci* 6: 1251-1252, 2003.
- Dayan P, Abbott LF. *Theoretical Neuroscience: Computational and Mathematical Modeling of Neural Systems*. Cambridge, MA: The MIT Press, 2005.
- Felsen G, Dan Y. A natural approach to studying vision. *Nat Neurosci* 8: 1643-1646, 2005.
- Grzywacz NM, Amthor FR. Robust directional computation in on-off directionally selective ganglion cells of rabbit retina. *Vis Neurosci* 24: 647-661, 2007.
- Grzywacz NM, Amthor FR, Merwine DK. Necessity of acetylcholine for retinal directionally selective responses to drifting gratings in rabbit. *J Physiol* 512: 575-581, 1998a.
- Grzywacz NM, Merwine DK, Amthor FR. Complementary roles of two excitatory pathways in retinal directional selectivity. *Vis Neurosci* 15: 1119-1128, 1998b.
- Grzywacz NM, Tootle JS, Amthor FR. Is the input to a GABAergic or cholinergic synapse the sole asymmetry in rabbit's retinal directional selectivity? *Vis Neurosci* 14: 39-54, 1997.
- Hammond P, Smith AT. Directional tuning interactions between moving oriented and textured stimuli in complex cells of feline striate cortex. *J Physiol* 342: 35-49, 1983.
- He S, Levick WR. Spatial-temporal response characteristics of the on-off direction selective ganglion cells in the rabbit retina. *Neurosci Lett* 285: 25-28, 2000.
- Holub RA, Morton-Gibson M. Response of visual cortical neurons of the cat to moving sinusoidal gratings: response-contrast functions and spatiotemporal interactions. *J Neurophysiol* 46: 1244-1259, 1981.
- Hughes A. A schematic eye for the rabbit. *Vision Res* 12: 123-138, 1972.

- Ikeda H, Wright MJ. Spatial and temporal properties of ‘sustained’ and ‘transient’ neurones in area 17 of the cat’s visual cortex. *Exp Brain Res* 22: 363-383, 1975.
- Jacobs AL, Fridman G, Douglas RM, Alam NM, Latham PE, Prusky GT, Nirenberg S. Ruling out and ruling in neural codes. *Proc Natl Acad Sci USA* 106: 5936-5941, 2009.
- Kittila CA, Massey SC. Pharmacology of directionally selective ganglion cells in the rabbit retina. *J Neurophysiol* 77: 675-689, 1997.
- Levick WR. Receptive fields and trigger features of ganglion cells in the visual streak of the rabbit’s retina. *J Physiol* 188: 285-307, 1967.
- Levick WR, Oyster CW, Takahashi E. Rabbit lateral geniculate nucleus: sharpener of directional information. *Science* 165: 712-714, 1969.
- Merwine DK, Amthor FR, Grzywacz NM. Non-monotonic contrast behavior in directionally selective ganglion cells and evidence for its dependence on their GABAergic input. *Vis Neurosci* 15: 1129-1136, 1998.
- Nowak P, Gawne TJ, Dobbins AC, Amthor FR. Extraction of stimulus parameters from responses of directionally selective retinal ganglion cells (Abstract) [Online]. *Program No. 165.7. 2009 Neuroscience Meeting Planner*. Chicago, IL: Society for Neuroscience, 2009. http://www.sfn.org/skins/main/pdf/abstracts/am2009/poster_presentations/PosterPresentation_SunAM.pdf [9 Jul 2010].
- Ölveczky BP, Baccus SA, Meister M. Segregation of object and background motion in the retina. *Nature* 423: 401-408, 2003.
- Ölveczky BP, Baccus SA, Meister M. Retinal adaptation to object motion. *Neuron* 56: 689-700, 2007.
- Optimization Toolbox User’s Guide (Version 4.1)* [Online]. The MathWorks, Inc., Natick, MA, 2008. <http://www.mathworks.com/access/helpdesk/help/toolbox/optim/> [10 Nov 2008].
- Osborne LC, Palmer SE, Lisberger SG, Bialek W. The neural basis for combinatorial coding in a cortical population response. *J Neurosci* 28: 13522-13531, 2008.
- Oyster CW. The analysis of image motion by the rabbit retina. *J Physiol* 199: 613-635, 1968.
- Oyster CW, Barlow HB. Direction-selective units in rabbit retina: distribution of preferred directions. *Science* 155: 841-842, 1967.
- Poggio T, Reichardt WE. Considerations on models of movement detection. *Kybernetik* 13: 223-227, 1973.

- Pouget A, Dayan P, Zemel R. Information processing with population codes. *Nat Rev Neurosci* 1: 125-132, 2000.
- Rapela J, Felsen G, Touryan J, Mendel JM, Grzywacz NM. ePPR: a new strategy for the characterization of sensory cells from input/output data. *Network* 21: 35-90, 2010.
- Risner ML, Amthor FR, Gawne TJ. The response dynamics of rabbit retinal ganglion cells to simulated blur. *Vis Neurosci* 27: 43-55, 2010.
- Schachter MJ, Oesch N, Smith RG, Taylor WR. Dendritic spikes amplify the synaptic signal to enhance detection of motion in a simulation of the direction-selective ganglion cell. *PLoS Comput Biol* 6: 1-24, 2010.
- Sclar G, Maunsell JH, Lennie P. Coding of image contrast in central visual pathways of the macaque monkey. *Vision Res* 30: 1-10, 1990.
- Sincich LC, Park KF, Wohlgemuth MJ, Horton JC. Bypassing V1: a direct geniculate input to area MT. *Nat Neurosci* 7: 1123-1128, 2004.
- Stern E, Aertsen A, Vaadia E, Hochstein S. Stimulus encoding by multidimensional receptive fields in single cells and cell populations in V1 of awake monkey. In: *Adv Neural Inf Process Syst* 5, edited by Hanson SJ, Cowan JD, Giles CL. San Mateo, CA: Morgan Kaufmann, 1993, p. 377-384.
- Strang CE, Renna JM, Amthor FR, Keyser KT. Nicotinic acetylcholine receptor expression by directionally selective ganglion cells. *Vis Neurosci* 24: 523-533, 2007.
- Taylor WR, He S, Levick WR, Vaney DI. Dendritic computation of direction selectivity by retinal ganglion cells. *Science* 289: 2347-2350, 2000.
- Taylor WR, Vaney DI. Diverse synaptic mechanisms generate direction selectivity in the rabbit retina. *J Neurosci* 22: 7712-7720, 2002.
- Tolhurst DJ, Movshon JA. Spatial and temporal contrast sensitivity of striate cortical neurones. *Nature* 257: 674-675, 1975.
- van Hateren JH. Directional tuning curves, elementary movement detectors, and the estimation of the direction of visual movement. *Vision Res* 30: 603-614, 1990.
- Wyatt HJ, Daw NW. Directionally sensitive ganglion cells in the rabbit retina: specificity for stimulus direction, size, and speed. *J Neurophysiol* 38: 613-626, 1975.
- Zeck GM, Masland RH. Spike train signatures of retinal ganglion cell types. *Eur J Neurosci* 26: 367-380, 2007.

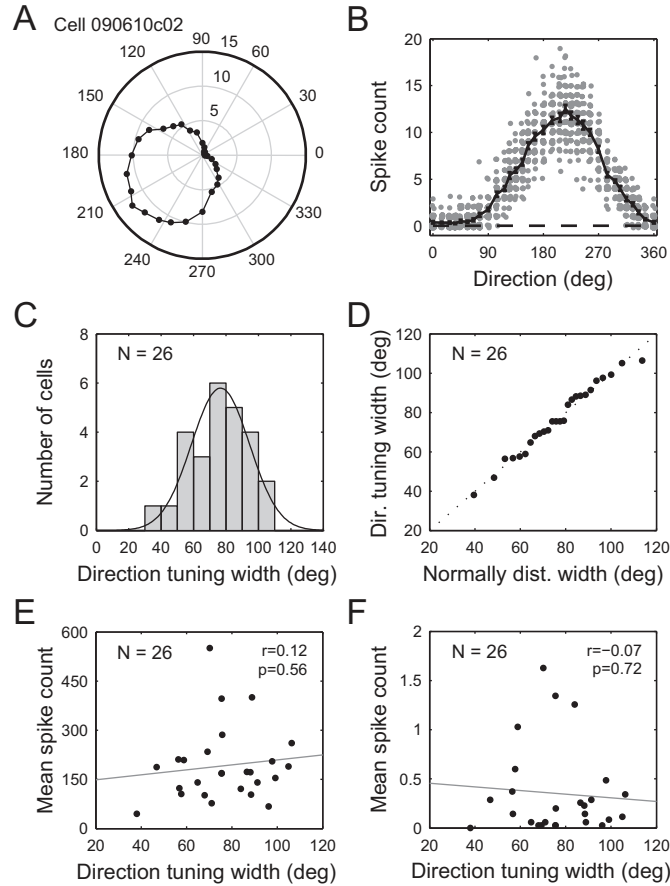


Figure 1. Direction tuning curves and their widths.

Direction tuning curves were determined from rabbit On-Off directionally selective retinal ganglion cells (On-Off DS RGCs) at 32 directions separated by $\sim 11.25^\circ$ by averaging spike counts from 35 trials per direction. Stimulus was a bar of luminance of 57.58 cd/m^2 swept at the speed of 2.84 mm/s as measured on the retina.

A. Polar plot of a representative direction tuning curve determined from a typical On-Off DS RGC. Tuning width computed as the half width at half maximum of a Gaussian fit was 75.5° .

B. Cartesian plot of the same direction tuning curve (black solid line) superimposed on spike counts from individual trials (gray dots). Positions of the dots are slightly jittered for better visibility. Bars on the curve show SE. For reference, mean number of spikes for no-stimulus (blank) condition is also shown (black broken line at the bottom).

C. Histogram of the direction tuning widths for each of the 26 cells. Each width was computed as the half width at half maximum of a Gaussian fit to the cell mean spike counts. Bin width is 10° , and the highest bin occurs between $70\text{--}80^\circ$. Overlying line represents the theoretical scaled normal distribution with the same mean and SD as those calculated from the data.

D. Quantile-quantile plot comparing the distribution of the direction tuning widths for the 26 cells to the theoretical scaled normal distribution with the same mean and SD. Line representing the identity relationship (dotted black) is shown as a reference.

E. Plot of the total of the mean spike counts being a sum over all directions vs. the direction tuning width for each of the 26 cells.

F. Plot of the mean spike counts for no stimulus (blank) condition vs. the direction tuning widths for the 26 cells.

In *E* and *F*, the linear regression line (solid gray) is shown for reference and the linear correlation coefficient (r) is quantified.

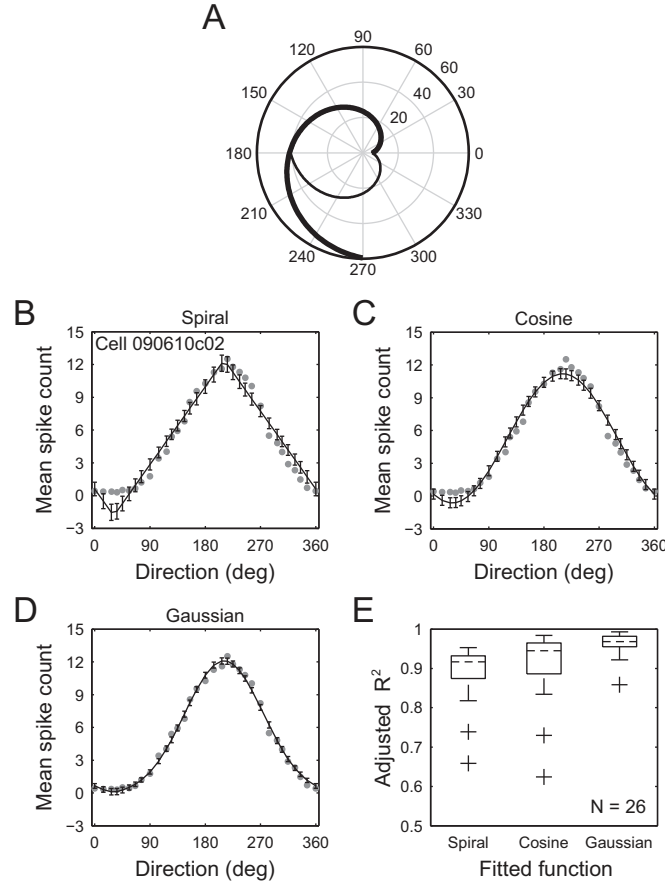


Figure 2. Functional approximation of direction tuning curves.

Direction tuning curves determined at 32 directions were fitted with 3 functions.

A. Polar plot of an example mirror-symmetric Archimedes' spiral function (with arbitrary parameter values). This function combines two standard Archimedes' spiral functions, one of which (black thin line) is shown over 180° , while the other is shown over 270° (black thick line). When both of the component functions are confined to 180° (a single hemi-plane) and symmetrically merged around the preferred direction, they form a mirror-symmetric Archimedes' spiral function, which has a cardioid shape.

B, C, D. Fits of the 3 functions: mirror-symmetric Archimedes' spiral (*B*), cosine (*C*), and Gaussian (*D*) (black lines) to the mean spike counts (gray dots) producing the direction tuning curve of a typical cell (the same as in Fig. 1, *A* and *B*). Bars on each line show 95% confidence intervals of the fitted function.

E. Box plot showing the spread of a measure of goodness of fit (adjusted R^2) for the 3 functions for the 26 cells. Central broken line in each box represents the median, the solid edges represent the first (bottom) and third (top) quartiles, and the whiskers extend to the most extreme values not considered outliers, whereas potential outliers are individually plotted as crosses.

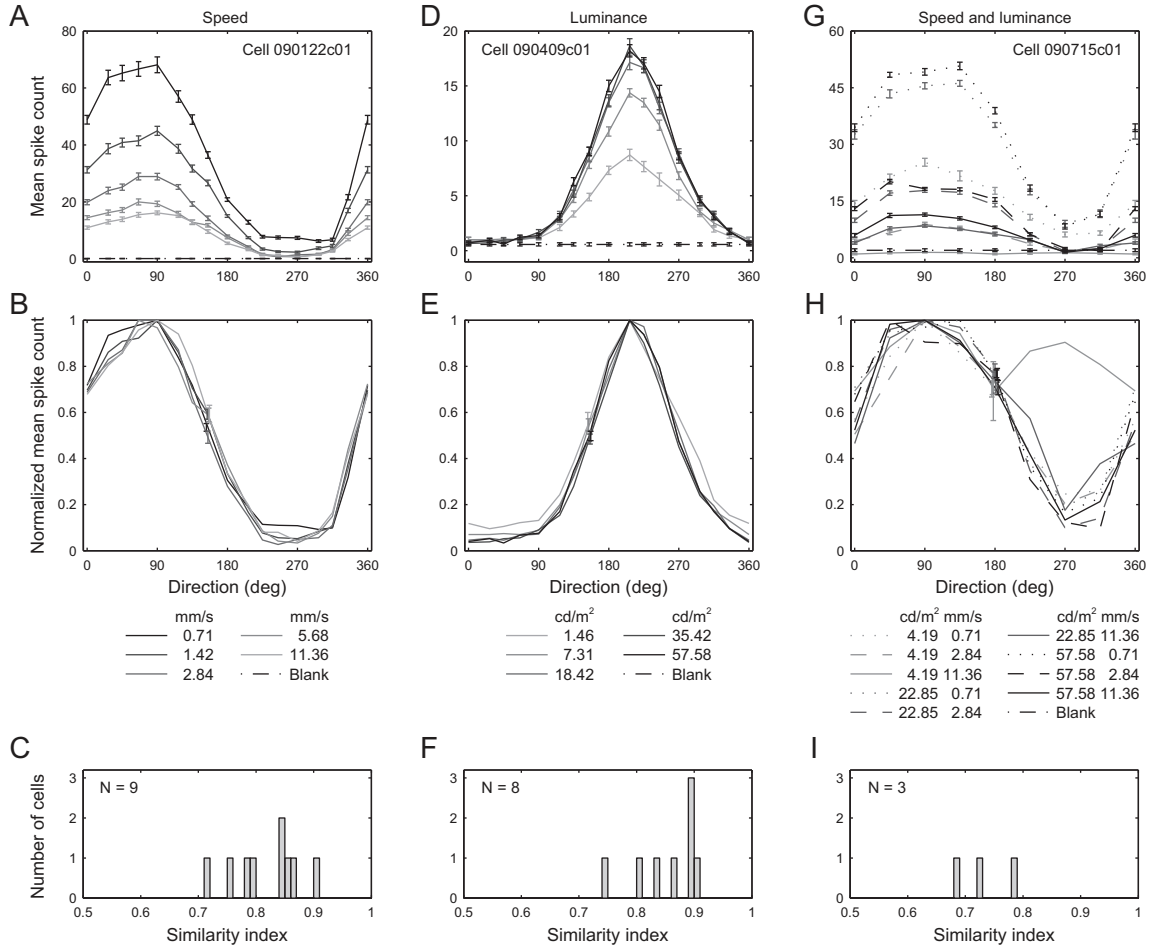


Figure 3. Invariance of direction tuning curves.

Direction tuning curves were determined either for different speeds (measured in mm/s on the retina), or for different luminance levels (measured in cd/m²), or for different combinations of both.

A. Direction tuning curves of the least noisy cell for five speeds. Curves (solid lines) were determined at 16 directions separated by $\sim 22.5^\circ$ for a bar of the luminance of 57.58 cd/m².

B. Same direction tuning curves after normalization with reference to the peak of each curve. Similarity index is 0.90.

C. Histogram of similarity indexes quantified for normalized direction tuning curves determined for different speeds for each of the 9 analyzed cells. Bin width is 0.01 unit, and the highest bin occurs between 0.84–0.85.

D. Direction tuning curves of one of the least noisy cells for five luminance levels. Curves (solid lines) were determined at 16 directions separated by $\sim 22.5^\circ$ for a bar swept at the speed of 2.84 mm/s.

E. Same direction tuning curves after normalization with reference to the peak of each curve. Similarity index is 0.90.

F. Histogram of similarity indexes quantified for normalized direction tuning curves determined for different luminance levels for each of the 8 analyzed cells. Bin width is 0.01 unit and the highest bin occurs between 0.89 and 0.90.

G. Direction tuning curves of the least noisy cell for the 9 combinations of 3 speeds and 3 luminance levels. Curves (solid, broken, and dotted lines) were determined for a bar at 8 directions separated by $\sim 45^\circ$.

H. Same direction tuning curves after normalization with reference to the peak of each curve. Similarity index is 0.79.

I. Histogram of similarity indexes quantified for normalized direction tuning curves determined for different combinations of speeds and luminance levels for each of the 3 cells. Bin width is 0.01 unit and the similarity indexes are 0.69, 0.72 and 0.79, respectively.

In *A*, *D*, and *G*, mean number of spikes for no-stimulus (blank) condition is shown as a reference (broken line with dots), while bars on each line show SE. In *B*, *E*, and *H*, bars on the lines show normalized SE, but for a better visibility they are shown only for a single direction and are slightly jittered along the abscissa.

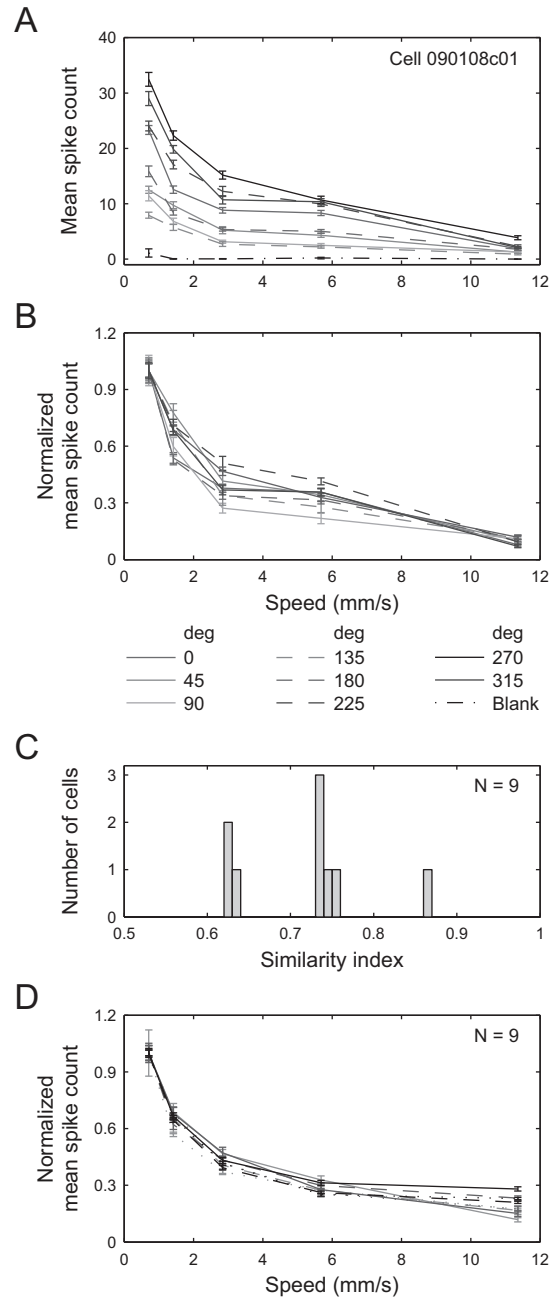


Figure 4. Speed tuning curves and their invariance.

Speed tuning curves were determined for five speeds (measured in mm/s on the retina) from the same data that were used for the investigation of invariance of direction tuning curves.

A. Speed tuning curves for 8 almost equidistant directions (reported as an angle in degrees) for the least noisy cell. For reference, mean number of spikes for no-stimulus (blank) condition is also shown (broken line with dots at the bottom).

B. Same speed tuning curves after normalization with reference to the peak of each curve. Similarity index is 0.86.

C. Histogram of similarity indexes quantified for normalized speed tuning curves determined for different directions for each of the 9 analyzed cells. Bin width is 0.01 unit, and the highest bin occurs between 0.73 and 0.74.

D. Normalized speed tuning curves for the preferred directions of the 9 analyzed cells. For each curve, normalization was carried out with reference to its peak. In *A*, bars on the lines show SE, while in *B* and *D*, they show normalized SE.

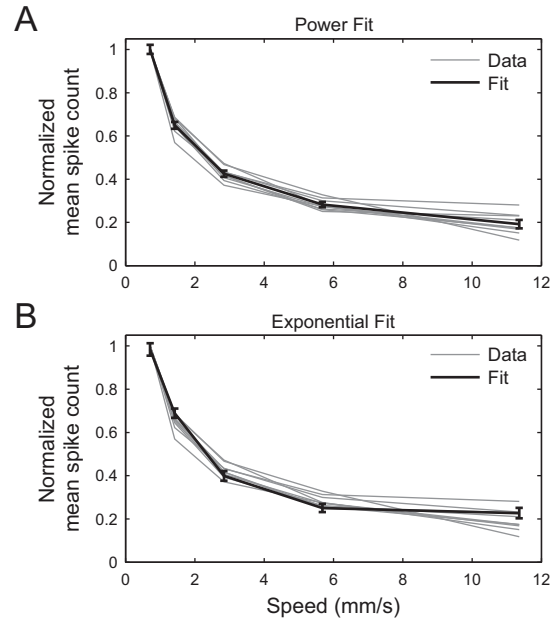


Figure 5. Functional approximation of speed tuning curves.

A, B. Normalized speed tuning curves for the preferred directions of the 9 analyzed cells (gray lines, the same data as in Fig. 4D) were fitted with two functions: power (*A*) and exponential decay (*B*) (black lines). Bars on each line representing a fit show 95% confidence intervals of the fitted function.

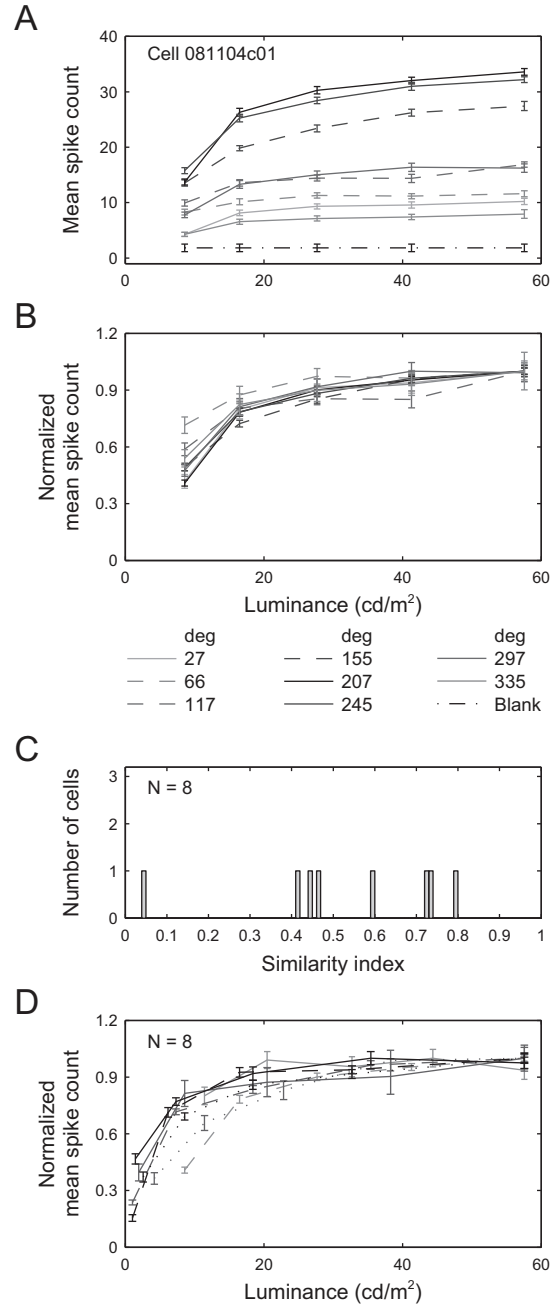


Figure 6. Luminance tuning curves and their invariance.

Luminance tuning curves were determined for five luminance levels (measured in cd/m²) from the same data that were used for the investigation of invariance of direction tuning curves.

A. Luminance tuning curves for 8 almost equidistant directions (reported as an angle in degrees) for the least noisy cell. For reference, mean number of spikes for the no-stimulus (blank) condition is also shown (broken line with dots at the bottom).

B. Same luminance tuning curves after normalization with reference to the peak of each curve. Similarity index is 0.80.

C. Histogram of similarity indexes quantified for normalized luminance tuning curves determined for different directions for each of the 8 analyzed cells. Bin width is 0.01 unit and there is no dominant value.

D. Normalized luminance tuning curves for the preferred directions of the 8 analyzed cells. For each curve, normalization was carried out with reference to its peak. In *A*, bars on the lines show SE, while in *B* and *D*, they show normalized SE.

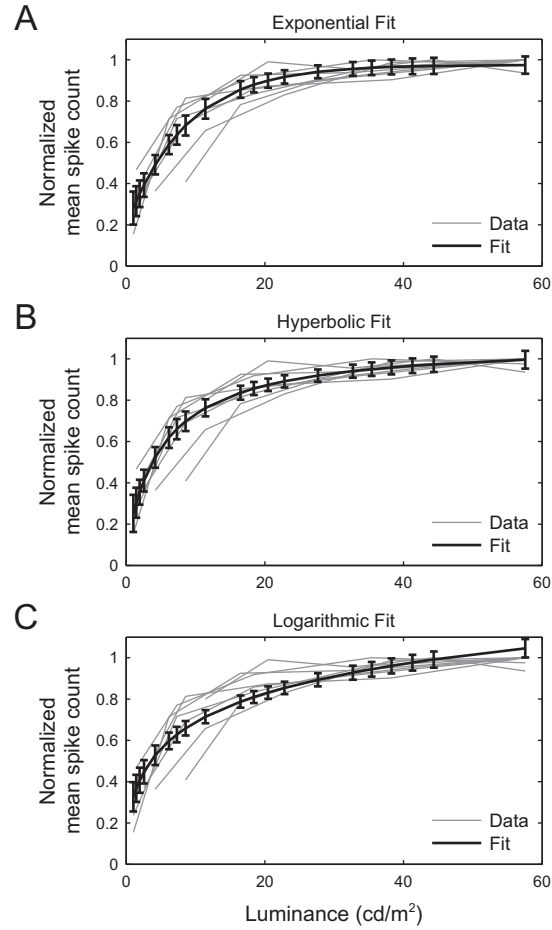


Figure 7. Functional approximation of luminance tuning curves.

A, B, C. Normalized luminance tuning curves for the preferred directions of the 8 analyzed cells (gray lines, the same data as in Fig. 6D) were fitted with 3 functions: exponential rise (*A*), rectangular hyperbola (*B*), and logarithmic (*C*) (black lines). Bars on each line representing a fit show 95% confidence intervals of the fitted function.

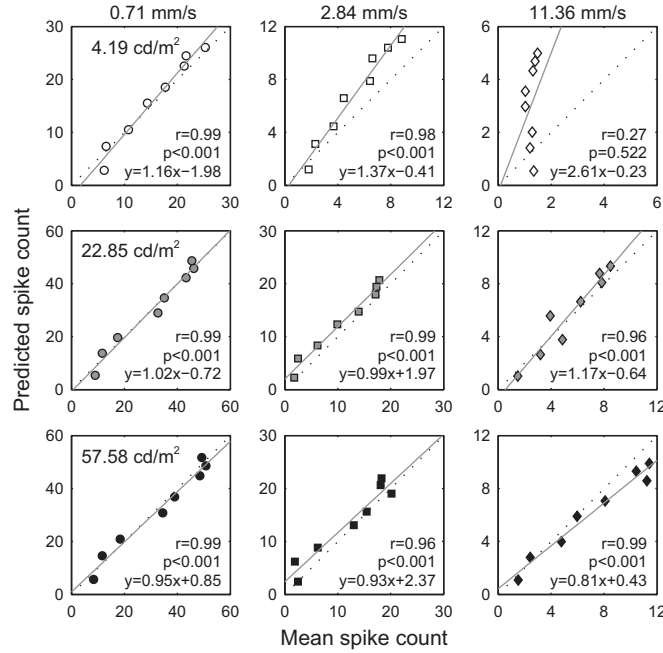


Figure 8. Prediction of spike count when direction, speed, and luminance are covaried. Predictions were obtained for one cell (the same as in Fig. 3, *G* and *H*) for the 9 combinations of 3 speeds (measured in mm/s on the retina) and 3 luminance levels (measured in cd/m²) based on the same data that were used for the investigation of invariance of direction tuning curves. For every combination, 8 predictions were computed, each corresponding to a different tested direction. Individual plots of the predicted spike counts vs. the mean spike counts for each combination are displayed in a 3×3 grid in which speeds vary across columns and luminance levels vary across rows. Corresponding speed is shown above the *top* plot of every column whereas the corresponding luminance level is shown in the *top left* corner of every plot on the left. Speeds are also distinguished by different marker shapes, and the luminance levels are distinguished by different marker colors. In each plot, both the linear regression line (solid gray) and the line representing the identity relationship (dotted black) are shown as a reference, and the linear correlation coefficient (r) is quantified.

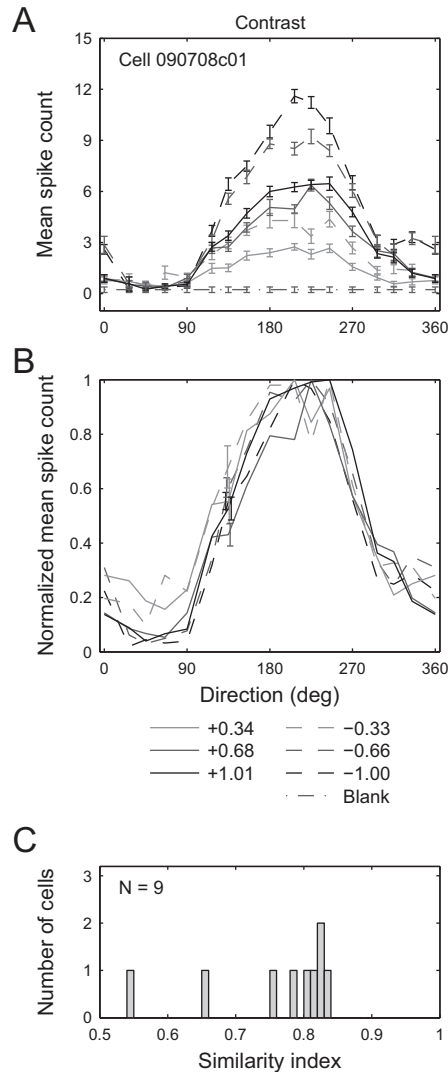


Figure 10. Invariance of direction tuning curves with respect to sign of contrast.

Direction tuning curves were determined for 3 positive and 3 negative contrasts (calculated as Weber contrasts) at 16 directions separated by $\sim 22.5^\circ$ for a bar swept at the speed of 2.84 mm/s against a mid-gray background of luminance 28.62 cd/m².

A. Direction tuning curves (solid lines) of the least noisy cell. Mean number of spikes for no-stimulus (blank) condition is shown as a reference (broken line with dots). Bars on each line show SE.

B. Same direction tuning curves after normalization with reference to the peak of each curve. Bars on the lines show normalized SE, but for a better visibility they are shown only for a single direction and are slightly jittered along the abscissa. Similarity index is 0.84.

C. Histogram of similarity indexes quantified for normalized direction tuning curves determined for different contrasts for each of the 9 cells. Bin width is 0.01 unit, and the highest bin occurs between 0.82–0.83.

INDEPENDENT CODING OF DIRECTION AND SPEED IN DIRECTIONALLY
SELECTIVE RETINAL GANGLION CELLS

by

PRZEMYSŁAW NOWAK, FRANKLIN R. AMTHOR, TIMOTHY J. GAWNE,
ALLAN C. DOBBINS

In preparation for *Nature*

Format adapted for dissertation

ABSTRACT

The nature of neural coding has been a topic of intense interest from the earliest days of sensory physiology (Adrian 1928; Hartline 1940) to the present day (Barlow 1961; Field and Chichilnisky 2007; Lettvin et al. 1959; Rieke et al. 1999). On-Off direction selective retinal ganglion cells (On-Off DS RGC) pose a particular challenge because their firing rate depends on stimulus direction as well as on nondirectional parameters such as speed and contrast. While On-Off DS RGCs reliably distinguish direction on the preferred-null axis independent of speed and contrast (Barlow and Hill 1963; Barlow et al. 1964; Barlow and Levick 1965; Grzywacz and Amthor 2007), it is not known how they represent direction and speed in general. Here, we show that direction and speed are encoded in different aspects of the spike train. At slow to medium speeds, On-Off DS RGCs exhibit a firing mode characterized by alternation of short and long interspike intervals — a spike doublet is followed by a longer interdoubtlet interval, and the length of the interdoubtlet interval varies systematically with speed. Strikingly, this pattern is invariant with direction. Therefore, a burst interval encoding is used to represent stimulus speed. In contrast, the integrated spike rate is a separable product of speed, direction, and luminance (Nowak et al. 2011). Since the luminance and speed functions are shared among On-Off DS RGCs, stimulus direction can be computed from the ratio of responses of a local population of these cells. This implies a duplex code in which central neurons can employ two different filters for motion decoding: a high pass

filter optimized for sensitivity to variation in the interdoublet interval to estimate speed and a low pass filter followed by ratiometric normalization to estimate direction.

Visual motion detection is ubiquitous in animals, and motion detection circuits have been among the most extensively studied in neuroscience (Borst and Euler 2011; Clifford and Ibbotson 2002). One group of neurons devoted to signaling motion comprises directionally selective (DS) cells, which occur across a wide range of species, from flies to vertebrates (Borst and Euler 2011; Clifford and Ibbotson 2002; Vaney et al. 2012). Their responses are most vigorous to a stimulus moving in one particular, or preferred, direction, and gradually decline to minimum for the opposite, or null, direction. Many mammals contain at least two types of DS cells in the retina (Demb 2007; Vaney et al. 2012), and here we focus on one of them, On-Off DS RGCs, which we investigated in rabbits. These cells respond to both leading and trailing edges of a light bar (Barlow and Levick 1965; Kittila and Massey 95), respond to a wide range of speeds (Grzywacz and Amthor 2007; Sivyer et al. 2010; Wyatt and Daw 1975), and prefer local motions due to a strong suppressive surround (Barlow et al. 1964; Barlow and Levick 1965; Chiao and Masland 2003). Moreover, they form four subclasses, each preferring a different cardinal direction (Oyster and Barlow 1967) and tiling the whole retina (Amthor and Oyster 1995; Vaney 1994). Consequently, each point in the field of view is projected onto the receptive fields of just four On-Off DS RGCs. Their responses, however, also depend on other stimulus parameters, such as speed (Grzywacz and Amthor 2007; Sivyer et al. 2010; Wyatt and Daw 1975) and contrast (Grzywacz and Amthor 2007; Merwine et al. 1998). As a result, for several parameters, including both direction and speed, these cells exhibit broad tuning curves (Fig. 1, *A* and *B*).

Because On-Off DS RGCs project to the lateral geniculate nucleus (LGN) (Levick et al. 1969; Pu and Amthor 1990), their output is presumably relayed to the cortex. However, LGN synapses are known to exhibit strong frequency-dependent filtering (Kara and Reid 2003; Sincich et al. 2007; Usrey et al. 1998), thus a low spike rate produced by a stimulus motion with nonoptimal parameters may not be transmitted by the LGN synapse. A possible solution to this problem could be provided by burst firing. Figure 1C shows the spike raster for an On-Off DS RGC responding to a thin bar stimulus swept across its receptive field in the preferred direction at a slow speed. There is no obvious macrostructure across trials apart from the bar entering and exiting the receptive field, and even the beginning of response is not precisely aligned. However, zooming into a 300 ms period (Fig. 1C, lower) reveals that the firing pattern is characterized by spike doublets separated by longer gaps and accompanied by occasional isolated spikes and triplets. There is clearly no doublet alignment across trials, which implies that the absolute time of occurrence is not significant. Figure 1D depicts the interspike interval (ISI) distribution for the same data, which exhibits a bimodal pattern, with the short ISI peak (~5 ms) reflecting the ISI within the spike doublet and the long ISI peak (~21 ms) reflecting the interval between successive doublets. This distribution is dramatically different from a Poisson spiking process due to the gap between the short and long ISI peaks. Figure 1E illustrates the relation between successive spikes in the joint ISI distribution (or return map), where spikes are represented in the plane by their preceding and succeeding ISIs. The concentration of spikes near the two axes indicates the alternation between the short and long ISIs, further confirmed for a single trial by

displaying the complete sequence of ISIs (Fig. 1*F*), which exhibits clear fluctuations between small and large values.

One interpretation of the doublet-gap-doublet firing pattern may be that the doublet represents a reliable spike. Studies in both cats (Kara and Reid 2003; Usrey et al. 1998) and monkeys (Sincich et al. 2007) have demonstrated that the probability of spike transmission at LGN synapses depends strongly on ISI. From the latter paper, one can estimate that the efficacy for a spike occurring 5 ms after the previous spike is about 70% greater than for a spike that occurs 40 ms after the previous spike. It should be mentioned, though, that neither of these studies involved DS cells, and that the characteristic of the LGN synapse at DS cell is not known. On the other hand, an early study observed that On-Off DS cells in the LGN have narrower direction tuning curves than their precursors in the retina, which was postulated as being due to an opponent process in the LGN (Levick et al. 1969). However, narrowing of the direction tuning curve might also be explained by synaptic filtering favoring bursts over isolated spikes.

We examined the spike pattern structure as stimulus speed was varied, and found that the intradoublet interval was constant, while the interdoublet interval varied with speed. This is illustrated both via the ISI distributions (Fig. 2*A*, left column) and the joint ISI distributions (Fig. 2*A*, right column) for a different cell than the one shown in Fig. 1. For each doubling of speed, the second distribution moves an approximately constant amount to the left, implying a logarithmic compression in the encoding of speed. From the joint ISI distributions, with increasing speed there is a progressive reduction in the long-long ISI pairs as the response becomes more concentrated in the lower left of the diagram. Although not explicitly shown here, there is a weak trend for burst length to

increase with increasing speed: singletons and doublets are most common at the slowest speeds, but supradoublet bursts become more frequent at higher speeds (data not shown). To quantify the effect of speed on the ISI distribution, we fitted the ISI distributions with the sum of two Gaussians and compared the location parameters corresponding to the intradoublet (G1) and interdoublet (G2) intervals. Figure 2*B* illustrates the distribution of these parameters for a sample of nine cells. G1 (left) is very similar across all cells (4–5 ms) independent of speed, while G2 (right) decreases with speed (the median drops ~5 ms per octave) until the fastest speed where the reduction is smaller.

We know that both spike rate and spike count fall off smoothly away from the preferred direction, so it is natural to suppose that the spike pattern would reflect this. Instead, as Fig. 3*A* shows, the intradoublet-interdoublet statistics do not change as direction is varied. Note that the number of spikes declines from the preferred to orthogonal direction (top to bottom) as does the ratio of short to long ISIs. The joint ISI distributions seem to show that as the stimulus direction is further from the preferred, there is a decline in the ratio of the short-long ISI alternations to the long-long ISI pairs. Consequently, there is a change in both spike number and spike pattern away from the preferred direction. Despite this, Fig. 3*B* shows that for the sample of On-Off DS RGCs, the locations of the short and long ISI peaks are invariant with direction. Therefore, unlike the overall spike rate and spike count, which vary with direction, the short-long alternation pattern faithfully signals stimulus speed.

Most of the experiments were performed with a thin bar, which raises a question: could spike doublets be an artifact of the spatiotemporal contiguity of the leading and trailing edges? The fact that the intradoublet interval (4–6 ms) was invariant with speed

suggests that the doublet cannot be directly explained in terms of leading and trailing edge responses. However, because On-Off DS RGCs have a bistratified dendritic field with On and Off inputs segregated into distinct sublaminae within the inner plexiform layer (Amthor et al. 1984), it might be postulated that excitation of both On and Off dendrites creates a distinctive mode of activation. To evaluate this, for one cell we performed the experiment using a block-like thick bar yielding separate On and Off responses. The spike statistics (G1 and G2 position) were in the middle of the thin bar sample (data not shown), which indicates that doublets are not an artifact of a special choice of stimulus. However, the broader question of the range of stimuli that elicit doublet spike patterning has not yet been systematically addressed.

It is also natural to ask whether the burst interval pattern remains constant as other nonmotion parameters are varied. One of these is stimulus luminance. As luminance is varied, On-Off DS RGCs exhibit a rapidly saturating response (Barlow and Hill 1963; Merwine et al. 1998; Nowak et al. 2011). Consequently, over a very broad range of luminances, response changes minimally with luminance. In experiments in which luminance was varied, we found that luminance affected interburst interval on the rapidly ascending arm of the luminance curve but not elsewhere. For stimuli between the firing threshold and the knee of the curve, luminance acts like increasing speed in that it decreases the interburst interval.

Figure 3 indicates that while the short-long intervals were invariant, other changes appeared away from the preferred direction. Figure 4A shows how ISI changed with speed and direction for three single trials in a format similar to Fig. 1F. The top row illustrates the sequence of ISIs for all spikes in one trial for the slowest speed tested in the

preferred direction, the middle row shows a trial for the fastest speed tested in the preferred direction, and the bottom row shows a trial for the slowest speed in the orthogonal direction. The top row shows the now-familiar short-long ISI structure. At the fastest speed in the preferred direction almost all the ISIs are short, and there are about a third as many spikes, while in the orthogonal direction at the slowest speed, in addition to the short-long alternations, there are some very long ISIs, and about half the number of spikes compared to the top row. The occurrence of both ISI persistence between 10–40 ms and the introduction of very long ISIs (>40 ms) reduces the spike count by half. To quantify the changes of ISI statistics, we partitioned the joint ISI distribution into a 3×3 array, and counted the ISIs in each array cell (Fig. 4A, right column; illustrated by gray scale). Compared with the slowest speed-preferred direction condition (top), where most joint ISIs are alternating, at the fastest speed the response is concentrated in the lower left cell, reflecting the continuous high firing rate. For the orthogonal-to-preferred direction and the slowest speed condition, the central cell (10–40, 10–40 ms) is the most populous, but there is a substantial increase in the very long joint ISI cells. We observe that a small number of very long ISIs can play a disproportionate role in controlling the low-pass filtered firing rate.

To examine the change in the joint ISI distribution with speed and direction, we clustered the 3×3 array into three categories: high firing rate, ISI alternations, and long and very long joint ISIs. Figure 4B (left) shows how the proportions of high firing rate, alternations, and isolated spikes vary with speed in the preferred direction. From the slowest to fastest speed, long-short alternations drop from slightly less than 60% to a little more than 20%, while the proportion of high rate spikes goes from negligible to

almost 70%. When varying direction at the slowest speed, the high rate is always negligible, but the alternations drop (again to ~20%), and the isolated spikes rise from 40% to 80%. Changes of speed affect the high frequency information: interdoublet intervals decrease until they merge into a single burst, while change of direction decreases the frequency of transmission of the burst interval message through insertion of long and very long ISI isolated spikes.

This strongly suggests a duplex coding scheme in which the high frequency information (interdoublet interval) conveys speed information and a low-pass filtered rate (equivalently, moving average) conveys a signal that is a function of the product of direction and speed (and luminance when on the rising arm of the luminance curve). There are a variety of methods available for decoding the direction signal from the quartet of On-Off DS RGCs, including taking ratios of orthogonal cell responses, because the luminance and speed tuning curves are very similar across the population and because the spike count is a separable product of the direction, speed, and luminance tuning functions (Nowak et al. 2011). The conditions meet those necessary for equivariance decoding (van Hateren 1990), and in network simulations with single trial data we have found that accurate directional decoding can be achieved independent of direction (in preparation).

This paper shows that On-Off DS RGCs in rabbit retina employ a burst interval spike patterning scheme in which the gap between bursts is related to the stimulus speed. The interburst interval is logarithmic in the stimulus speed, which represents a tradeoff: a loss of speed resolution to permit increased directional resolution. Note that there is an

economy achieved by using the duration of absence of spikes rather than presence of spikes between the doublets.

The mechanism of doublet firing is unknown, although it has been observed in many different systems. In simulations of RGCs, doublets were observed under certain conditions and explained by independent spike initiation at separate loci in the trigger zone (Fohlmeister and Miller 1997). Alternatively, the doublet-interdoublet pattern could be due to an interaction between voltage-dependent Ca^{++} and $\text{K}(\text{Ca}^{++})$ or $\text{Cl}(\text{Ca}^{++})$ channels triggered by Ca^{++} entry and eliciting a doublet-dependent afterhyperpolarization (DDAHP). The DDAHP would produce the interdoublet gap, and if stimulus speed modulates excitation, for example via the number of dendritic Ca^{++} spikes (Oesch et al. 2005), stimulus speed would modulate recovery from the DDHP and hence the interdoublet interval. The exponential DDAHP could thus produce the compressive speed coding observed. Speed can be decoded with a suitable high-pass filter. Possible mechanisms are both presynaptic (e.g., paired-pulse facilitation) and postsynaptic (e.g., NMDA bursts in cortical pyramidal cell fine dendrites occur for short ISI pairs (Polsky et al. 2009)). Because On-Off DS RGCs are not velocity-selective in the strongest sense, i.e., not clearly oriented in spatiotemporal frequency space (Grzywacz and Amthor 2007; He and Levick 2000), it is not yet clear the range of stimuli/conditions over which On-Off DS RGCs can reliably report speed. For instance, strong surround suppression may restrict reliable speed coding to small objects — such as potential predators at a distance. While further work is needed to examine the range of stimuli that elicit doublet burst firing and the precision with which speed can be decoded, we find it intriguing that a variety of other direction selective neurons are known to exhibit burst firing such as in

the cercal ganglion of the cricket (Aldworth et al. 2011) and electrosensory neurons of the weakly electric fish (Khosravi-Hashemi et al. 2011), which may reflect both energetic and computational economies in motion coding.

METHODS SUMMARY

We reanalyzed data published previously (Nowak et al. 2011). All experimental procedures were approved by the University of Alabama at Birmingham Institutional Animal Care and Use Committee. Briefly, small weight New Zealand albino rabbits (1.6–4.2 kg) of both sexes were anesthetized initially with urethane (intraperitoneal injection) followed by Nembutal (marginal ear vein injection), and their eyes were enucleated. Extracellular recordings from single On-Off DS RGCs were obtained from the eyecup preparation superfused with heated (33–35°C), oxygenated, bicarbonate-buffered Ames medium. Stimuli were displayed on a CRT monitor (refresh rate: 100 Hz) and projected onto the retina. Either a thin or a thick bright bar (luminance: 57.58 cd/m², irradiance: 9.73 μW/cm²) moving perpendicular to its long side was swept on a dark background (luminance: 0 cd/m², irradiance: 0.57 μW/cm²) across the receptive field in 16 directions separated by ~22.5° at 5 speeds between 0.71 mm/s (4.10°/s) and 11.36 mm/s (65.66°/s) with doubling increments (conversion based on the retinal magnification factor of 0.173 mm/° (Hughes 1972)). Each recording comprised 35 trials, in each of which all stimulus configurations were arranged in a shuffled random order. Signal waveform was Schmitt triggered, and spikes were extracted on-line to the nearest millisecond by a custom-made application. Subsequently, the data were analyzed offline using MATLAB 7.12 (MathWorks, Natick, MA). Fits of sum-of-two-Gaussians to interspike interval histograms were obtained with MATLAB Optimization Toolbox (ver. 6.0) utilizing trust-region reflective Newton algorithm.

REFERENCES

- Adrian ED. *The Basis of Sensation: The Action of the Sense Organs*. New York, NY: W.W. Norton & Co., 1928.
- Aldworth ZN, Dimitrov AG, Cummins GI, Gedeon T, Miller JP. Temporal encoding in a nervous system. *PLoS Comput Biol* 7: e1002041, 2011.
- Amthor FR, Oyster CW. Spatial organization of retinal information about the direction of image motion. *Proc Natl Acad Sci USA* 92: 4002-4005, 1995.
- Amthor FR, Oyster CW, Takahashi ES. Morphology of on-off direction-selective ganglion cells in the rabbit retina. *Brain Res* 298: 187-190, 1984.
- Barlow HB. Possible principles underlying the transformations of sensory messages. In: *Sensory Communication*, edited by Rosenblith W. Cambridge, MA: The MIT Press, 1961, p. 217-234.
- Barlow HB, Hill RM. Selective sensitivity to direction of movement in ganglion cells of the rabbit retina. *Science* 139: 412-414, 1963.
- Barlow HB, Hill RM, Levick WR. Retinal ganglion cells responding selectively to direction and speed of image motion in the rabbit. *J Physiol* 173: 377-407, 1964.
- Barlow HB, Levick WR. The mechanism of directionally selective units in rabbit's retina. *J Physiol* 178: 477-504, 1965.
- Borst A, Euler T. Seeing things in motion: models, circuits, and mechanisms. *Neuron* 71: 974-994, 2011.
- Chiao CC, Masland RH. Contextual tuning of direction-selective retinal ganglion cells. *Nat Neurosci* 6: 1251-1252, 2003.
- Clifford CWG, Ibbotson MR. Fundamental mechanisms of visual motion detection: models, cells and functions. *Prog Neurobiol* 68: 409-437, 2002.
- Demb JB. Cellular mechanisms for direction selectivity in the retina. *Neuron* 55: 179-186, 2007.
- Field GD, Chichilnisky EJ. Information processing in the primate retina: circuitry and coding. *Annu Rev Neurosci* 30: 1-30, 2007.

- Fohlmeister JF, Miller RF. Mechanisms by which cell geometry control repetitive impulse firing in retinal ganglion cells. *J Neurophysiol* 78: 1948-1964, 1997.
- Grzywacz NM, Amthor FR. Robust directional computation in on-off directionally selective ganglion cells of rabbit retina. *Vis Neurosci* 24: 647-661, 2007.
- Hartline HK. The receptive fields of optic nerve fibers. *Am J Physiol* 130: 690-699, 1940.
- He S, Levick WR. Spatial-temporal response characteristics of the ON-OFF direction selective ganglion cells in the rabbit retina. *Neurosci Lett* 285: 25-28, 2000.
- Hughes A. A schematic eye for the rabbit. *Vision Res* 12: 123-138, 1972.
- Kara P, Reid RC. Efficacy of retinal spikes in driving cortical responses. *J Neurosci* 23: 8547-8557, 2003.
- Khosravi-Hashemi N, Fortune ES, Chacron MJ. Coding movement direction by burst firing in electrosensory neurons. *J Neurophysiol* 106: 1954-1968, 2011.
- Kittila CA, Massey SC. Effect of ON pathway blockade on directional selectivity in the rabbit retina. *J Neurophysiol* 73: 703-712, 1995.
- Lettvin JY, Maturana HR, McCulloch WS, Pitts WH. What the frog's eye tells the frog's brain. *Proc Inst Radio Engrs* 47: 1940-1951, 1959.
- Levick WR, Oyster CW, Takahashi E. Rabbit lateral geniculate nucleus: sharpener of directional information. *Science* 165: 712-714, 1969.
- Merwine DK, Amthor FR, Grzywacz NM. Non-monotonic contrast behavior in directionally selective ganglion cells and evidence for its dependence on their GABAergic input. *Vis Neurosci* 15: 1129-1136, 1998.
- Nowak P, Dobbins AC, Gawne TJ, Grzywacz NM, Amthor FR. Separability of stimulus parameter encoding by on-off directionally selective rabbit retinal ganglion cells. *J Neurophysiol* 105: 2083-2099, 2011.
- Oesch N, Euler T, Taylor WR. Direction-selective dendritic action potentials in rabbit retina. *Neuron* 47: 739-750, 2005.
- Oyster CW, Barlow HB. Direction-selective units in rabbit retina: distribution of preferred directions. *Science* 155: 841-842, 1967.
- Polsky A, Mel B, Schiller J. Encoding and decoding bursts by NMDA spikes in basal dendrites of layer 5 pyramidal neurons. *J Neurosci* 29: 11891-11903, 2009.

Pu ML, Amthor FR. Dendritic morphologies of retinal ganglion cells projecting to the lateral geniculate nucleus in the rabbit. *J Comp Neurol* 302: 675-693, 1990.

Rieke F, Warland D, de Ruyter van Steveninck R, Bialek, W. *Spikes: Exploring the Neural Code*. Cambridge, MA: The MIT Press, 1999.

Sincich LC, Adams DL, Economides JR, Horton JC. Transmission of spike trains at the retinogeniculate synapse. *J Neurosci* 27: 2683-2692, 2007.

Sivyer B, van Wyk M, Vaney DI, Taylor WR. Synaptic inputs and timing underlying the velocity tuning of direction-selective ganglion cells in rabbit retina. *J Physiol* 588, 3243-3253, 2010.

Usrey WM, Reppas JB, Reid RC. Paired-spike interactions and synaptic efficacy of retinal inputs to the thalamus. *Nature* 395: 384-387, 1998.

van Hateren JH. Directional tuning curves, elementary movement detectors, and the estimation of the direction of visual movement. *Vision Res* 30: 603-614, 1990.

Vaney DI. Territorial organization of direction-selective ganglion cells in rabbit retina. *J Neurosci* 14: 6301-6316, 1994.

Vaney DI, Sivyer B, Taylor WR. Direction selectivity in the retina: symmetry and asymmetry in structure and function. *Nat Rev Neurosci* 13: 194-208, 2012.

Wyatt HJ, Daw NW. Directionally sensitive ganglion cells in the rabbit retina: specificity for stimulus direction, size, and speed. *J Neurophysiol* 38: 613-626, 1975.

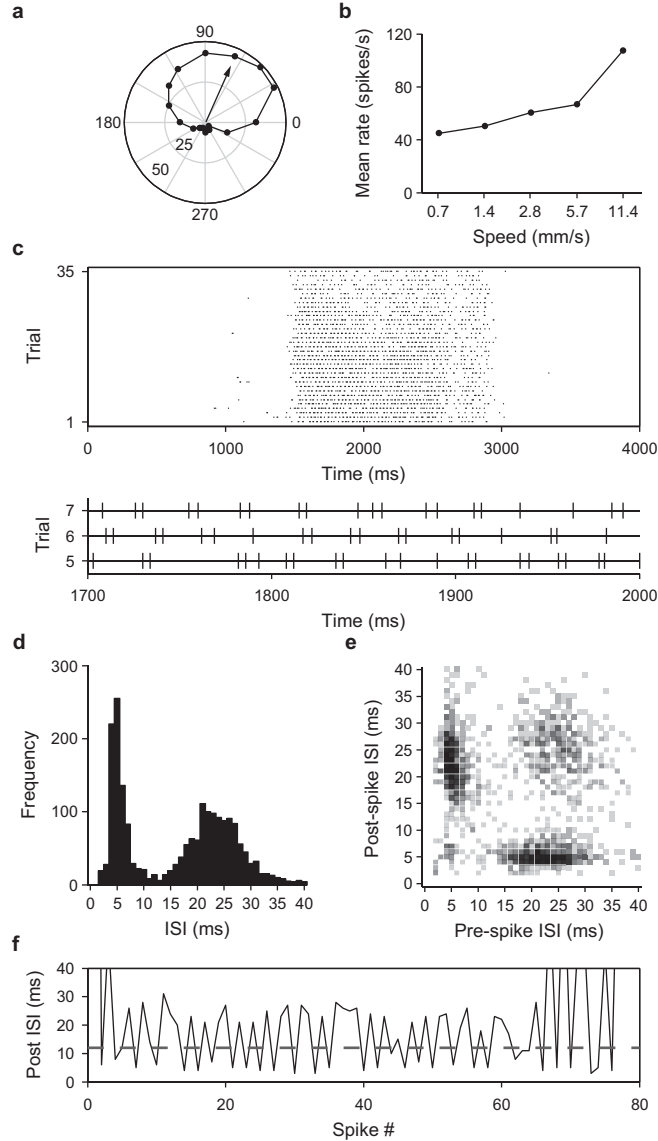


Figure 1. On-Off DS cell response to motion.

A. Characteristic broad direction tuning curve (obtained at a low speed, 0.7 mm/s on the retina, 4.1°/s; thin bar moved in 16 directions). The arrow indicates the preferred direction (pooled estimate from tuning curves at 5 speeds).

B. Speed tuning curve obtained for a bar swept in the preferred direction.

C. Raster plot of individual spikes (preferred direction, lowest speed) for all 35 trials (*top*), and a magnification of a 300 ms segment of 3 trials (*bottom*). Note recurring alternations between short and long interspike intervals (ISIs).

D. Bimodal ISI histogram for the data in *C* (bin width, 1 ms). ISIs longer than 40 ms were infrequent and are not shown.

E. Density plot of joint ISIs for the same responses, with darker squares representing larger counts. Note two clusters corresponding to alternations between short (~5 ms) and long (~22 ms) ISIs, which accords with the two peaks of the ISI histogram (shown in *D*).

F. Complete sequence of ISIs for one trial (trial 6). The pattern clearly exhibits recurring alternations between short and long ISIs. [Horizontal broken line (12 ms) is a boundary between the two peaks in the ISI histogram.]

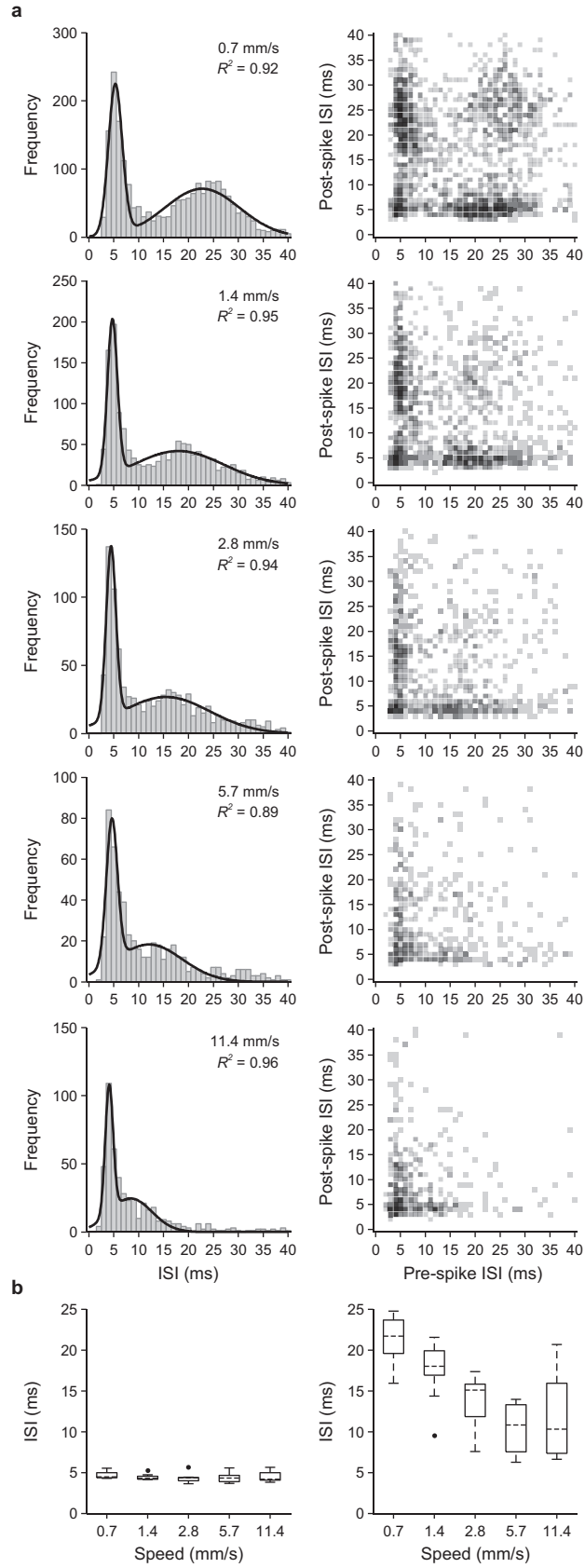


Figure 2. Interburst interval decreases with increasing speed.

A. ISI histograms of a cell obtained for the preferred direction at 5 speeds (*left column*) and the corresponding density plots of joint ISIs (*right column*). As speed increases, the second peak (interdoublet gap) in the ISI histograms shifts toward and eventually merges with the first peak, while the location of the first peak (intradoublet gap) remains constant. Solid lines superimposed on the ISI histograms show fits of sums of two Gaussians. Goodness-of-fit measured as R^2 was high (0.89–0.96). Maximum counts in different joint ISI density plots varied (8–18), and color code is relative. Likewise, in the joint ISI plots, as speed increases the two clusters representing short-long alternations move to the lower left corner and then merge.

B. Distribution of the first (*left*) and second (*right*) location parameters of the two Gaussians fitted to the ISI histograms obtained from 9 analyzed cells. Solid boxes represent interquartile ranges, broken lines denote medians, and whiskers extend to the most extreme values not considered outliers, while outliers are depicted as dots. The location of the first Gaussian component is constant across speeds and cells with little variation, while the location of the second component moves toward that of the first one as speed increases (consistent with plots shown in *A*). Relatively higher variation in the locations of the second component at the highest speed is due to imperfect fits in some cells resulting from merging of the two peaks and low spike count.

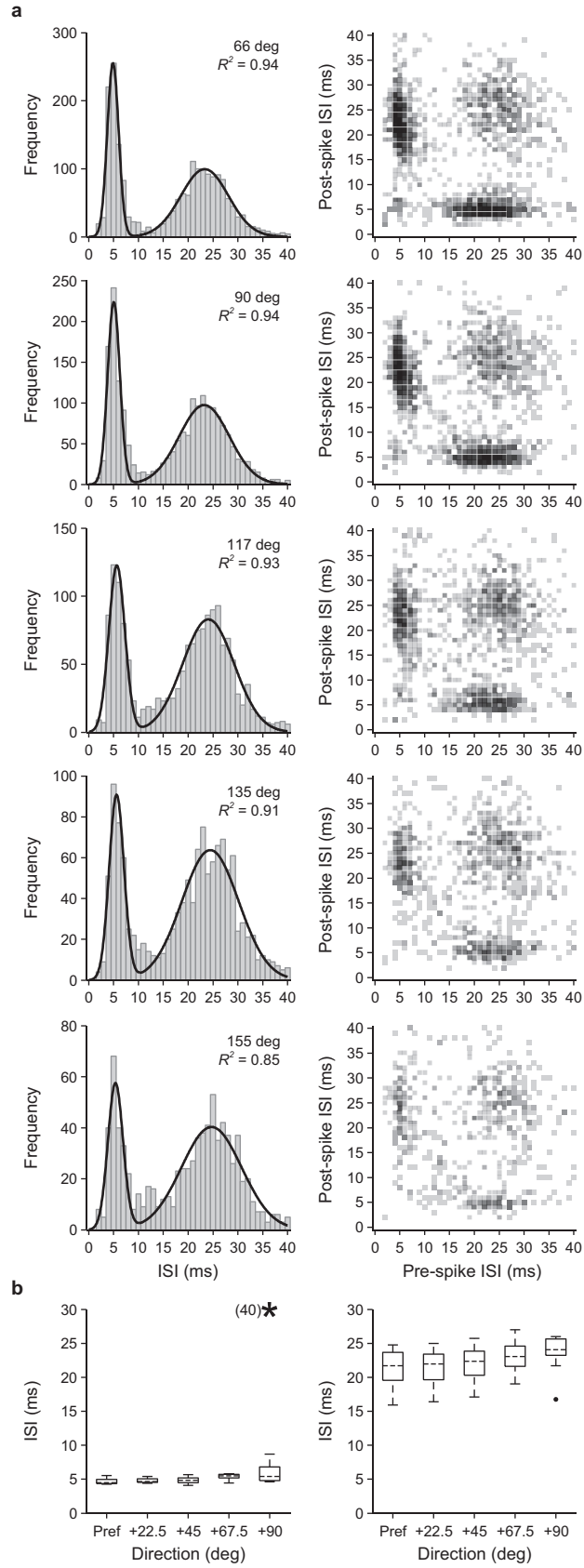


Figure 3. Doublet pattern is invariant with direction.

A. ISI histograms as direction is varied from the preferred to orthogonal direction (*left column*) and the corresponding joint ISI density plots (*right column*). The locations of both ISI peaks are constant across directions as are the locus of doublets (short-long ISI alternations). (Same cell as in Figure 1; speed, 0.7 mm/s; 5 directions.) Solid lines on ISIs show sum of Gaussian fits. Goodness of fit was high (R^2 range, 0.85–0.94).

B. Fits for all 9 cells confirm that the interdoubt interval is invariant with direction. (Symbols same as in Figure 2.) There is very little variability in the first location and slightly greater in the other. The outlier (star – *left plot*; dot – *right plot*) occurred in a cell in which the fit did not converge properly due to weak response/high noise in the orthogonal-to-preferred direction.

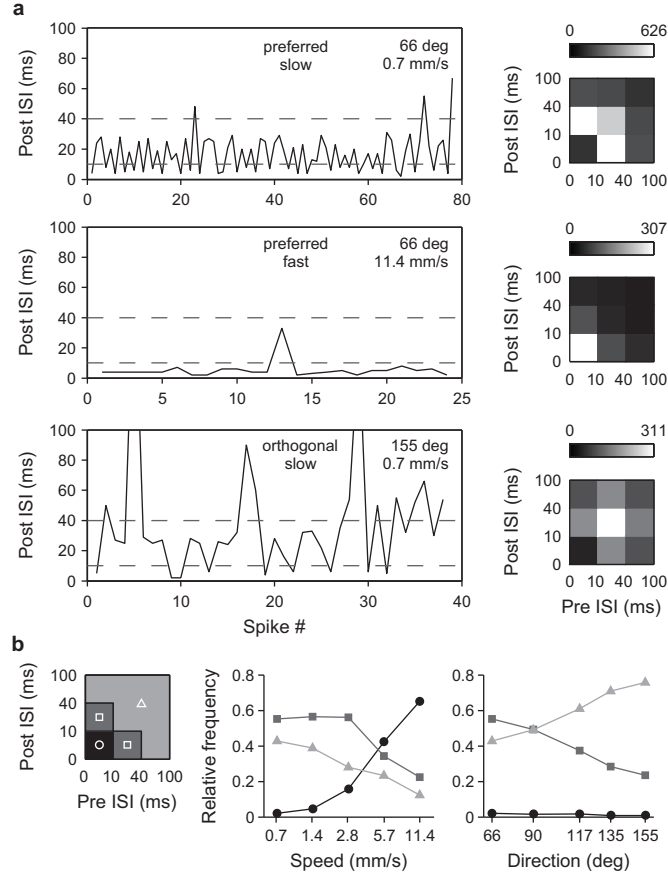


Figure 4. Effect of speed and direction on spike pattern.

A. ISI sequences from individual trials (*left column*) and partitioned joint ISIs (*right column*). The joint ISIs are binned into 3x3 arrays (see text). *Top*: slow speed, preferred direction – predominance of doublets; *middle*: fast, preferred – long burst with one interpolated long ISI; *bottom*: slow, orthogonal – doublets are interrupted by long (10–40 ms) and very long (>40 ms) ISIs. Broad directional tuning is created by the insertion of the long ISIs into the response. (Same cell as in Figs. 1 and 3.)

B. Contribution of bursts, doublets, and long ISIs to spike pattern. *Left*: a three way partition into supradoublet bursts (lower left cell), short-long alternation (two cells adjoining the burst cell), and long ISIs (the remaining 6 cells). The array color coding is carried over to the two graphs. *Middle*: with increasing speed, the fraction of doublets declines as the fraction of longer bursts increases. *Right*: as direction moves away from the preferred, the fraction of doublets declines and the fraction of isolated spikes increases.

DISCUSSION

This dissertation was motivated by an apparent paradox shown by responses of On-Off DS RGCs: on the one hand, these cells exhibit precise direction discrimination along the preferred-null axis, independent of many nondirectional parameters, such as speed and contrast, but on the other hand, those nondirectional parameters, characterized by broad direction tuning curves, also affect the responses, which thus become ambiguous. Consequently, it was not clear what information on the moving stimulus is actually conveyed by these cells and how this information is encoded.

Since the response of On-Off DS RGCs is determined by more than one stimulus parameter, it seems possible that the role of these cells is to transmit information on more parameters than just the stimulus direction. One particularly interesting combination involves both the stimulus direction and speed, which together yield velocity. A hypothesis that On-Off DS RGCs signal velocity is attractive because it would allow the higher visual centers to use these cells' output in optic flow computations.

To address the problem of what information is encoded by On-Off DS RGCs and in what form, this dissertation investigated the effects of different stimulus parameters on different measures of these cells' responses.

As a result, several findings have been made. The first study, which examined a first-order measure of response, the mean spike count, has shown that the effects of direction, speed, and luminance on the response are multiplicatively separable. It has also confirmed that the response falls off in a gradual manner from the maximum at the

preferred direction to the minimum at the null direction (Barlow et al. 1964), and has demonstrated that this relationship is best captured by the Gaussian function, although the cosine function has been found to offer a close fit as well. Moreover, it has confirmed a nonlinear effect of speed: as speed increases, the response decreases, with a rapid decrease at slow speeds followed by a slower decrease at fast speeds (Wyatt and Daw 1975), and it has shown that this relationship is well fitted by the power function. It has also confirmed that an increase in luminance results in a nonlinear increase in response, with a rapid increase at low luminance values that flattens out at high luminance values (Merwine et al. 1998), and it has demonstrated that the exponential rise function well approximates this association. Moreover, this study has also determined that the speed and luminance tuning curves appear universal across On-Off DS RGCs throughout the retina. All these results suggest that at any retinal location the effects of nondirectional parameters could be normalized out in a divisive manner by means of population coding, thus permitting accurate direction estimation. The second study, in turn, focused on a second-order measure of response, the interspike intervals. It has demonstrated that direction, speed, and luminance are represented in different aspects of the spike train, which gives rise to characteristic burst patterns. It has shown that the intraburst interval is constant independent of stimulus configuration, while the interburst interval is strongly modulated by nondirectional parameters, especially speed, but not by direction. These results suggest that direction and nondirectional parameters could be simultaneously extracted using different filters.

Altogether, this research has addressed some aspects of the nature of the neural code employed by On-Off DS RGCs. The problem of the neural code involves two

components: encoding and decoding (Dayan and Abbott 2005). Encoding constitutes a forward problem that seeks an answer to the following question: given the stimulus, what will be the cell response? Decoding, in contrast, is an inverse problem described by the opposite question: given the response, what was the stimulus that elicited it? This dissertation has dealt only with the problem of stimulus encoding, and has used different measures of response in the two studies. Decoding, on the other hand, has not been addressed, and until it happens, the picture remains incomplete. To make it complete, it needs to be quantitatively shown what stimulus parameters can be successfully estimated from responses of On-Off DS RGCs and what estimation accuracy can be achieved.

The results of the first study indicate that mean spike count responses of On-Off DS RGCs satisfy the assumptions for isotropic assessment of the stimulus direction described by van Hateren (1990). Consequently, it should be possible to estimate direction using a first-order measure of responses of a local population comprising four orthogonally-tuned On-Off DS RGCs, and moreover, the error of such estimates should be direction-independent. These conclusions, however, must be validated with experiments or simulations. Such a test should aim at answering several questions. First, is it actually possible to determine direction from population responses? If so, the next question should concern the accuracy of estimation. Is the accuracy equal for all directions, as predicted from the theoretical considerations of van Hateren (1990), or is it different for different directions? A similar question should be asked with respect to nondirectional parameters: is the accuracy independent of nondirectional parameters, or is it, for instance, smaller for those producing weaker responses, as the latter are inherently more susceptible to noise? Estimation accuracy should also be examined in

terms of choice of the decoding method. Since extracting stimulus parameters from population responses is a complex problem, several decoding methods have been devised for this purpose. One of them is the population vector proposed by Georgopoulos et al. (1982). It is a linear method in which direction estimate is computed using a weighted sum of the preferred directions of the cells in the population, with weights determined based on the magnitude of cell responses. It has been successfully applied, for instance, to prediction of direction of arm movements in monkeys, in which case responses of neurons in the motor cortex were utilized (Georgopoulos et al. 1982). Although simple and widely accepted, from the perspective of estimation accuracy this method may not be optimal (Dayan and Abbott 2005). Methods that offer optimal accuracy, such as the maximum likelihood method, have been derived from a probabilistic approach (Sanger 1996). They take into account not only the current population response, but also the distribution of these responses across trials, which results in more accurate estimations. However, these distributions must be determined in advance, which presents an additional requirement. In the case of direction estimation from population responses of On-Off DS RGCs, it necessitates quantification of the response variability for various combinations of directions and nondirectional parameters. Another aspect addressed by a test validating possibility of direction decoding from population responses of these cells should concern the temporal evolution of response. It is conceivable that traversal of a stimulus across the receptive field does not have to complete before the stimulus direction can be extracted, which may be especially important when the traversal time is long, for example at slow speeds. Therefore, it should be determined how estimation accuracy improves as the response develops, and what is the minimum duration needed

for the accuracy to be adequate. A final question that the test should answer pertains to the stimulus form. Given that natural scenes are rather complex, is it possible to estimate stimulus direction not only for single bars, but also, for instance, for gratings or random dot patterns? And if so, is the accuracy of direction estimation independent of the stimulus form?

Some preliminary results based on simulations in which population responses of On-Off DS RGCs were synthesized from responses of single cells to a moving bar suggest that direction estimation by the population vector method is possible and yields sufficient accuracy (Fig. 1).

The results of the second study indicate that direction and nondirectional parameters are encoded in different aspects of the spike train, at least for some ranges of nondirectional parameter values, which gives rise to characteristic bursts. Interestingly, burst are also present in responses of DS cells in other systems and species, for instance in the cercal sensory system of the cricket (Aldworth et al. 2011) and in the electrosensory system of the weakly electric fish (Khosravi-Hashemi et al. 2011), although bursts in these systems may not necessarily share the same properties with bursts produced by On-Off DS RGCs. The finding that direction and nondirectional parameters are differently encoded by On-Off DS RGCs, again, entails new questions. First, is it possible to decode both direction and the nondirectional parameters from the same response by applying different filters? If so, is it possible to estimate individual values of the nondirectional parameters, or only the lumped effect can be assessed? The last question leads to a related one: is the pattern equally affected by all nondirectional parameters or maybe one of them, specifically speed, predominates? If individual

parameters can be estimated, or possibly only the dominant one, what is the estimation accuracy? Furthermore, can the patterning improve the accuracy of direction estimation beyond that based on the mean spike count? Will it be also present when textured stimuli rather than bars are used? And finally, what is the physiological mechanism underlying the patterning?

All the questions stemming from the results of the first and the second study should be further pursued. They will naturally lead to an answer to a more fundamental question: can the output of On-Off DS RGCs be used to compute optic flow? Importantly, both studies utilized spatially restricted stimuli rather than whole field motion. For textured flow stimuli, the suppressive surround of these cells will cause reduced responses. Will the information on direction and speed still be present in those weak responses?

Regardless of the answers, pursuing the above questions will unravel various mechanisms governing the signaling of On-Off DS RGCs, and hopefully help elucidate the function that this type of RGCs performs in the visual system. This dissertation has made a step in that direction.

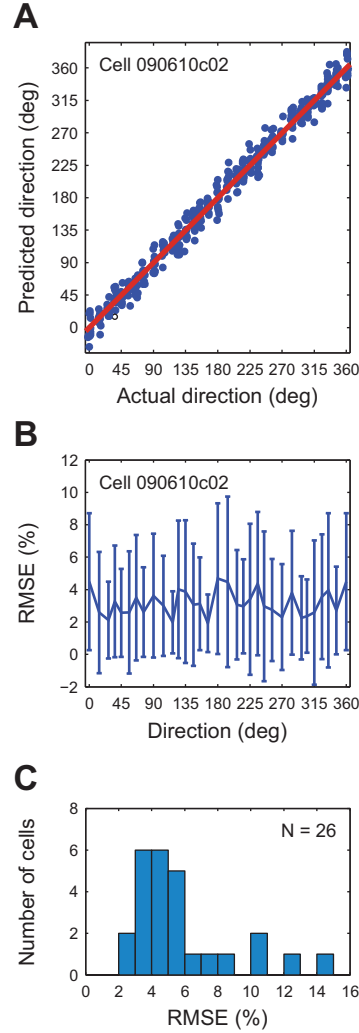


Figure 1. Direction prediction by the population vector.

Each population of 4 orthogonally tuned cells was simulated based on data from a different On-Off DS RGC by appropriate rotation of responses to 32 directions. Every simulated population response comprised a quartet of single trial spike counts chosen randomly from 35 trials, independently for each simulated cell. This sampling was repeated 12 times for each direction.

A. Comparison of the predicted vs. actual directions for an example cell. Individual predictions (blue dots) concentrate along the identity relationship (red line). Blue dot positions were slightly jittered for better visibility.

B. Root-mean-square error (RMSE) of predictions for individual directions for an example cell (the same as in *A*). RMSE is expressed as percent of 360°. Line connects mean error values for 12 replicates per direction, and bars represent SD. Errors appear to be isotropic over the full range of directions.

C. Histogram of mean RMSEs across all predictions for a sample of 26 cells. RMSE is expressed as percent of 360°, and the mean error value over all predictions was calculated individually for each cell. Bin width is 1%.

GENERAL LIST OF REFERENCES

- Aldworth ZN, Dimitrov AG, Cummins GI, Gedeon T, Miller JP. Temporal encoding in a nervous system. *PLoS Comput Biol* 7: e1002041, 2011.
- Amthor FR, Keyser KT, Dmitrieva NA. Effects of the destruction of starburst-cholinergic amacrine cells by the toxin AF64A on rabbit retinal directional selectivity. *Vis Neurosci* 19: 495-509, 2002.
- Amthor FR, Oyster CW. Spatial organization of retinal information about the direction of image motion. *Proc Natl Acad Sci USA* 92: 4002-4005, 1995.
- Amthor FR, Oyster CW, Takahashi ES. Morphology of on-off direction-selective ganglion cells in the rabbit retina. *Brain Res* 298: 187-190, 1984.
- Amthor FR, Takahashi ES, Oyster CW. Morphologies of rabbit retinal ganglion cells with concentric receptive fields. *J Comp Neurol* 280: 72-96, 1989a.
- Amthor FR, Takahashi ES, Oyster CW. Morphologies of rabbit retinal ganglion cells with complex receptive fields. *J Comp Neurol* 280: 97-121, 1989b.
- Ariel M, Daw NW. Effects of cholinergic drugs on receptive field properties of rabbit retinal ganglion cells. *J Physiol* 324: 135-160, 1982a.
- Ariel M, Daw NW. Pharmacological analysis of directionally sensitive rabbit retinal ganglion cells. *J Physiol* 324: 161-185, 1982b.
- Barlow HB. Action potentials from the frog's retina. *J Physiol* 119: 58-68, 1953.
- Barlow HB, Hill RM. Selective sensitivity to direction of movement in ganglion cells of the rabbit retina. *Science* 139: 412-414, 1963.
- Barlow HB, Hill RM, Levick WR. Retinal ganglion cells responding selectively to direction and speed of image motion in the rabbit. *J Physiol* 173: 377-407, 1964.
- Barlow HB, Levick WR. The mechanism of directionally selective units in rabbit's retina. *J Physiol* 178: 477-504, 1965.
- Borst A, Euler T. Seeing things in motion: models, circuits, and mechanisms. *Neuron* 71: 974-994, 2011.

- Bremmer F. Visual Neuroscience: the brain's interest in natural flow. *Curr Biol* 18: R263-R265, 2008.
- Caldwell JH, Daw NW. New properties of rabbit retinal ganglion cells. *J Physiol* 276: 257-276, 1978.
- Caldwell JH, Daw NW, Wyatt HJ. Effects of picrotoxin and strychnine on rabbit retinal ganglion cells: lateral interactions for cells with more complex receptive fields. *J Physiol* 276: 277-298, 1978.
- Chiao CC, Masland RH. Contextual tuning of direction-selective retinal ganglion cells. *Nat Neurosci* 6: 1251-1252, 2003.
- Cohen ED, Miller RF. Quinoxalines block the mechanism of directional selectivity in ganglion cells of the rabbit retina. *Proc Natl Acad Sci USA* 92: 1127-1131, 1995.
- Dayan P, Abbott LF. *Theoretical Neuroscience: Computational and Mathematical Modeling of Neural Systems*. Cambridge, MA: The MIT Press, 2005.
- Demb JB. Cellular mechanisms for direction selectivity in the retina. *Neuron* 55: 179-186, 2007.
- Elstrott J, Feller MB. Vision and the establishment of direction-selectivity: a tale of two circuits. *Curr Opin Neurobiol* 19: 293-297, 2009.
- Famiglietti EV. 'Starburst' amacrine cells and cholinergic neurons: mirror-symmetric on and off amacrine cells of rabbit retina. *Brain Res* 261: 138-144, 1983.
- Famiglietti EV. Dendritic co-stratification of ON and ON-OFF directionally selective ganglion cells with starburst amacrine cells in rabbit retina. *J Comp Neurol* 324: 322-335, 1992.
- Famiglietti EV. "Small-tufted" ganglion cells and two visual systems for the detection of object motion in rabbit retina. *Vis Neurosci* 22: 509-534, 2005.
- Fried SI, Münch TA, Werblin FS. Mechanisms and circuitry underlying directional selectivity in the retina. *Nature* 420: 411-414, 2002.
- Fried SI, Münch TA, Werblin FS. Directional selectivity is formed at multiple levels by laterally offset inhibition in the rabbit retina. *Neuron* 46: 117-127, 2005.
- Georgopoulos AP, Kalaska JF, Caminiti R, Massey JT. On the relations between the direction of two-dimensional arm movements and cell discharge in primate motor cortex. *J Neurosci* 2: 1527-1537, 1982.

Grzywacz NM, Amthor FR. Robust directional computation in on-off directionally selective ganglion cells of rabbit retina. *Vis Neurosci* 24: 647-661, 2007.

Grzywacz NM, Amthor FR, Merwine DK. Necessity of acetylcholine for retinal directionally selective responses to drifting gratings in rabbit. *J Physiol* 512: 575-581, 1998.

Harris MG. Optic and retinal flow. In: *Visual Detection of Motion*, edited by Smith AT, Snowden RJ. San Diego, CA: Academic Press Inc, 1994, p. 307-332.

Hartline HK. The response of single optic nerve fibers of the vertebrate eye to illumination of the retina. *Am J Physiol* 121: 400-415, 1938.

He S, Levick WR. Spatial-temporal response characteristics of the ON-OFF direction selective ganglion cells in the rabbit retina. *Neurosci Lett* 285: 25-28, 2000.

Hoshi H, Tian LM, Massey SC, Mills SL. Two distinct types of ON directionally selective ganglion cells in the rabbit retina. *J Comp Neurol* 519: 2509-2521, 2011.

Hughes A, Whitteridge D. The receptive fields and topographical organization of goat retinal ganglion cells. *Vision Res* 13: 1101-1114, 1973.

Jacobson M, Gaze RM. Types of visual response from single units in the optic tectum and optic nerve of the goldfish. *Q J Exp Physiol Cogn Med Sci* 49: 199-209, 1964.

Kanjhan R, Sivyer B. Two types of ON direction-selective ganglion cells in rabbit retina. *Neurosci Lett* 483: 105-109, 2010.

Khosravi-Hashemi N, Fortune ES, Chacron MJ. Coding movement direction by burst firing in electrosensory neurons. *J Neurophysiol* 106: 1954-1968, 2011.

Kittila CA, Massey SC. Effect of ON pathway blockade on directional selectivity in the rabbit retina. *J Neurophysiol* 73: 703-712, 1995.

Kittila CA, Massey SC. Pharmacology of directionally selective ganglion cells in the rabbit retina. *J Neurophysiol* 77: 675-689, 1997.

Kuffler SW. Discharge patterns and functional organization of mammalian retina. *J Neurophysiol* 16: 37-68, 1953.

Lappe M, Bremmer F, van den Berg AV. Perception of self-motion from visual flow. *Trends Cognit Sci* 3: 329-336, 1999.

Lee S, Kim K, Zhou ZJ. Role of ACh-GABA cotransmission in detecting image motion and motion direction. *Neuron* 68: 1159-1172, 2010.

- Levick WR. Receptive fields and trigger features of ganglion cells in the visual streak of the rabbit's retina. *J Physiol* 188: 285-307, 1967.
- Levick WR. Receptive fields of retinal ganglion cells. In: *Physiology of Photoreceptor Organs*, edited by Fuortes MGF. Berlin: Springer-Verlag, 1972, p. 531-566.
- Lewis JE, Kristan WB. Representation of touch location by a population of leech sensory neurons. *J Neurophysiol* 80: 2584-2592, 1998.
- Lipetz LE, Hill RM. Discrimination characteristics of the turtle's retinal ganglion cells. *Experientia* 26: 373-374, 1970.
- Mallot HA. *Computational Vision*. Cambridge, MA: The MIT Press, 2000.
- Masland RH. The fundamental plan of the retina. *Nat Neurosci* 4: 877-886, 2001.
- Masland RH, Ames A. Responses to acetylcholine of ganglion cells in an isolated mammalian retina. *J Neurophysiol* 39: 1220-1235, 1976.
- Massey SC, Miller RF. N-methyl-D-aspartate receptors of ganglion cells in rabbit retina. *J Neurophysiol* 63: 16-30, 1990.
- Maturana HR, Frenk S. Directional movement and horizontal edge detectors in the pigeon retina. *Science* 142: 977-979, 1963.
- Maturana HR, Lettvin JY, McCulloch WS, Pitts WH. Anatomy and physiology of vision in the frog (*Rana pipiens*). *J Gen Physiol* 43(6): 129-175, 1960.
- Merwine DK, Grzywacz NM, Tjepkes DS, Amthor FR. Non-monotonic contrast behavior in directionally selective ganglion cells and evidence for its dependence on their GABAergic input. *Vis Neurosci* 15: 1129-1136, 1998.
- Michael CR. Receptive fields of directionally selective units in the optic nerve of the ground squirrel. *Science* 152: 1092-1095, 1966.
- Miller JP, Jacobs GA, Theunissen FE. Representation of sensory information in the cricket cercal sensory system. I. Response properties of the primary interneurons. *J Neurophysiol* 66: 1680-1689, 1991.
- Oesch N, Euler T, Taylor WR. Direction-selective dendritic action potentials in rabbit retina. *Neuron* 47: 739-750, 2005.
- Oyster CW. The analysis of image motion by the rabbit retina. *J Physiol* 199: 613-635, 1968.

- Oyster CW, Amthor FR, Takahashi ES. Dendritic architecture of ON-OFF direction-selective ganglion cells in the rabbit retina. *Vision Res* 33: 579-608, 1993.
- Oyster CW, Barlow HB. Direction-selective units in rabbit retina: distribution of preferred directions. *Science* 155: 841-842, 1967.
- Pu ML, Amthor FR. Dendritic morphologies of retinal ganglion cells projecting to the nucleus of the optic tract in the rabbit. *J Comp Neurol* 302: 657-674, 1990a.
- Pu ML, Amthor FR. Dendritic morphologies of retinal ganglion cells projecting to the lateral geniculate nucleus in the rabbit. *J Comp Neurol* 302: 675-693, 1990b.
- Reichardt W. Autocorrelation, a principle for the evaluation of sensory information by the central nervous system. In: *Sensory Communication*, edited by Rosenblith WA. Cambridge, MA: MIT Press, 1961, p. 303-317.
- Rodieck RW. *The First Steps in Seeing*. Sunderland, MA: Sinauer Associates Inc., 1998.
- Sanger TD. Probability density estimation for the interpretation of neural population codes. *J Neurophysiol* 76: 2790-2793, 1996.
- Stone J, Fabian M. Specialized receptive fields of the cat's retina. *Science* 152: 1277-1279, 1966.
- Sun L, Han X, He S. Direction-selective circuitry in rat retina develops independently of GABAergic, cholinergic and action potential activity. *PLoS One* 6: e19477, 2011.
- Tauchi M, Masland RH. The shape and arrangement of the cholinergic neurons in the rabbit retina. *Proc R Soc Lond B Biol Sci* 223: 101-119, 1984.
- Taylor WR, Vaney DI. Diverse synaptic mechanisms generate direction selectivity in the rabbit retina. *J Neurosci* 22: 7712-7720, 2002.
- van Hateren JH. Directional tuning curves, elementary movement detectors, and the estimation of the direction of visual movement. *Vision Res* 30: 603-614, 1990.
- Vaney DI. Territorial organization of direction-selective ganglion cells in rabbit retina. *J Neurosci* 14: 6301-6316, 1994.
- Vaney DI, Peichl L, Wässle H, Illing RB. Almost all ganglion cells in the rabbit retina project to the superior colliculus. *Brain Res* 212: 447-453, 1981.
- Vaney DI, Sivyer B, Taylor WR. Direction selectivity in the retina: symmetry and asymmetry in structure and function. *Nat Rev Neurosci* 13: 194-208, 2012.

Wässle H. Parallel processing in the mammalian retina. *Nat Rev Neurosci* 5: 747-757, 2004.

Werblin FS. Response of retinal cells to moving spots: intracellular recording in *Necturus maculosus*. *J Neurophysiol* 33: 342-350, 1970.

Werblin FS. Lateral interactions at inner plexiform layer of vertebrate retina: antagonistic responses to change. *Science* 175: 1008-1010, 1972.

Werblin FS, Dowling JE. Organization of the retina of the mudpuppy, *Necturus maculosus*. II. Intracellular recording. *J Neurophysiol* 32: 339-355, 1969.

Wyatt HJ, Daw NW. Directionally sensitive ganglion cells in the rabbit retina: specificity for stimulus direction, size, and speed. *J Neurophysiol* 38: 613-626, 1975.

Wyatt HJ, Daw NW. Specific effects of neurotransmitter antagonists on ganglion cells in rabbit retina. *Science* 191: 204-205, 1976.

Yang G, Masland RH. Receptive fields and dendritic structure of directionally selective retinal ganglion cells. *J Neurosci* 14: 5267-5280, 1994.

Yoshida K, Watanabe D, Ishikane H, Tachibana M, Pastan I, Nakanishi S. A key role of starburst amacrine cells in originating retinal directional selectivity and optokinetic eye movement. *Neuron* 30: 771-780, 2001.

APPENDIX

INSTITUTIONAL ANIMAL CARE AND USE COMMITTEE APPROVAL FORM




THE UNIVERSITY OF ALABAMA AT BIRMINGHAM

Institutional Animal Care and Use Committee (IACUC)

NOTICE OF APPROVAL

DATE: May 18, 2010

TO: Gawne, Timothy J.
WORB-654 4390
934-5495

FROM: 
Judith A. Kapp, Ph.D., Chair
Institutional Animal Care and Use Committee

SUBJECT: Title: Visual Cortical and Retinal Electrophysiology in Rabbits
Sponsor: Internal
Animal Project Number: 100408433

On May 18, 2010, the University of Alabama at Birmingham Institutional Animal Care and Use Committee (IACUC) reviewed the animal use proposed in the above referenced application. It approved the use of the following species and numbers of animals:

Species	Use Category	Number in Category
Rabbits	B	50

Animal use is scheduled for review one year from April 2010. Approval from the IACUC must be obtained before implementing any changes or modifications in the approved animal use.

Please keep this record for your files, and forward the attached letter to the appropriate granting agency.

Refer to Animal Protocol Number (APN) 100408433 when ordering animals or in any correspondence with the IACUC or Animal Resources Program (ARP) offices regarding this study. If you have concerns or questions regarding this notice, please call the IACUC office at 934-7692.

Institutional Animal Care and Use Committee
CH19 Suite 403
933 19th Street South
205.934.7692
FAX 205.934.1188

Mailing Address:
CH19 Suite 403
1530 3RD AVE S
BIRMINGHAM AL 35294-0019

Experimental data collection using animals was completed in September 2009.